GLOBAL UNFOLDING OF CHUA's CIRCUITS

by

L. O. Chua

Memorandum No. UCB/ERL M93/7

1 January 1993

GLOBAL UNFOLDING OF CHUA'S CIRCUITS

by

L. O. Chua

Memorandum No. UCB/ERL M93/7

1 January 1993

ELECTRONICS RESEARCH LABORATORY

College of Engineering
University of California, Berkeley
94720

This work is supported in part by the Office of Naval Research under grant N00014-89-J-1402 and the National Science Foundation under grant MIP-9001336.

rich and complex dynamics of this simplest among all chaotic circuits.

1 *Introduction*

1.1 *Historical Background*

The circuit shown in Fig.1(a) was synthesized to be the *simplest* autonomous (i.e., no input signals) electronic circuit generator of *chaotic* signals. The history on the conception of this circuit and its systematic synthesis procedure are summarized in Ref.[1], which is based in part on the author's opening lecture given at the *Workshop on Nonlinear Theory and its Applications* (NOLTA' 92), held at Waseda University, Tokyo, in January 1992. The chaotic nature of this circuit was first verified by *computer simulation*[1] by Matsumoto, who named it *Chua's circuit* [2], and confirmed *experimentally* by Zhong and Ayrom [3]. The author was not involved in these two publications because shortly after he had designed the circuit of Fig.1, he was rushed to a hospital in Tokyo for major surgery, an illness that took him almost a year to recuperate.

A comprehensive mathematical analysis of Chua's circuit and the first rigorous proof of its chaotic property are given in Ref.[4]. Because Chua's circuit was, and still is, the only known physical system whose mathematical model is capable of duplicating all experimentally observed chaotic and bifurcation phenomena, and which has yielded to a rigorous mathematical proof, it has generated worldwide interests not only among electrical engineers, but also mathematicians and physicists, as evidenced by the extensive literature on this circuit (see the Chronological Bibliography in Section 7). These publications, which covers extensively the experimental, numerical, and mathematical aspects of this circuit, has made Chua's circuit the

[1]The episode leading to this event was vividly described in Ref.[1]. Matsumoto's role at that point in time was that of a programmer, implementing the instructions from the author. However, Matsumoto's strong leadership in relentlessly driving his entire team of students to crank out, by brute-force computer calculations, the cross section of the strange attractor had led to the prompt identification of its *double-spiral* structure. The subsequent eigenvalue and eigenspace calculations were made by Matsumoto, following the analysis made by Komuro.

GLOBAL UNFOLDING OF CHUA'S CIRCUITS

L. O. Chua*

Jan 1,1993

SUMMARY

By adding a small linear resistor in series with the inductor in Chua's circuit, we obtain a circuit whose state equation is ***topologically conjugate*** (i.e., equivalent) to a 21-parameter family $\mathcal{C}$ of continuous odd-symmetric piecewise-linear equations in $\mathcal{R}^3$. In particular, every system or vector field belonging to the family $\mathcal{C}$, can be *mapped* via an explicit non-singular linear transformation into this circuit, which is uniquely determined by 7 parameters. Since no circuit with less than 7 parameters has this property, this augmented circuit is called an *unfolding* of Chua's circuit—–it is analogous to that of "unfolding a vector field" in a small neighborhood of a singular point. Our unfolding, however, is *global* since it applies to the entire state space $\mathcal{R}^3$.

The significance of the *unfolded Chua's Circuit* is that the *qualitative dynamics* of every autonomous $3rd$-order chaotic circuit, system, and differential equation, containing one odd-symmetric 3-segment piecewise-linear function can be mapped into this circuit, thereby making their separate analysis unnecessary. This immense power of unification reduces the investigation of the many heretofore unrelated publications on chaotic circuits and systems to the analysis of only one *canonical* circuit. This unified approach is illustrated by many examples selected from a zoo of more than 30 strange attractors extracted from the literature. In addition, a gallery of 18 strange attractors in full color is included to demonstrate the immensely

*The author is with the Department of Electrical Engineering and Computer Sciences, University of California, Berkeley, CA 94720 USA.

best understood——in terms of its nonlinear dynamics——among all known chaotic systems, and has triggered an avalanche of recent research activities on the applications of chaos, as documented in a recent Special Session of the Midwest Symposium on Circuits and Systems devoted to "Chua's Circuits," [5] and in two Special Issues of the *Journal of Circuits, Systems, and Computers*, entitled, "Chua's circuit: A Paradigm for chaos", and edited by R. N. Madan [6]-[7].

1.2 *Recent Applications*

In spite of their extreme sensitivities to initial conditions, two identical Chua's circuits and/or their subcircuits, can be operated in phase *synchronization*, even when operating in a chaotic regime [8]-[9]. In addition, several methods have been developed for *controlling* chaos in Chua's circuit [10]-[15]. The possibility for synchronizing and controlling chaos has already been exploited in the design of secure communication systems [16]-[17]. Moreover, a new phenomenon called "Stochastic Resonance" has recently been discovered in Chua's circuit [18]-[19], which can be applied to design novel amplifiers whose output SNR (signal-to-noise ratio) is considerably *greater* than the input SNR, an impressive feat that can not be achieved by any *linear* amplifier whose output SNR is always less than that of the input because the internal amplifier noise will *degrade* the SNR further.

Although the nonlinear resistor in the circuit of Fig.1(a) can be easily built using only a dual op-amp package and 6 linear resistors [20]-[21], an integrated circuit version of this nonlinear device, powered by a single 9-V battery, has been built [22]. Therefore, even the nonlinear resistor in Fig.1(a) can be mass produced as off-the-shelf components for future large scale industrial applications.

1.3 *Recent generalizations*

Chua's circuit has recently been generalized in many directions. One direction simply substitutes the *piecewise-linear* function of the nonlinear resistor by a smooth function, such as a polynomial [23]. Another direction models Chua's circuit by various 1-D maps [24]-[25]. A third direction investigates a CNN (Cellular Neural Network) array of Chua's circuits [26]-[27]. Still another direction increases the dimension of the state space but retaining the single scalar nonlinearity. For example, Ref.[28] uses a finite number of discrete lossy transmission line sections as the resonator, Ref.[29] uses a terminated coaxial cable as the resonator, and Ref.[30] uses a delay line as the resonator. Yet another direction of generalization focuses on an in-depth mathematical characterization of the geometrical structure of the strange attractors [31]-[32]. All of these generalizations are fascinating and could give rise to many novel applications. For example, Ref.[33] uses a cubic nonlinearity and the normal form theory for low-level visual sensing, and Ref.[34] makes use of a delay-line resonator to synthesize novel tones and music.

2 *Strange Attractors from Chua's Circuit*

2.1 *Concept of Equivalence of Dynamic Nonlinear Circuits*

Table 1 shows 6 *non-periodic* attractors so far found from Chua's circuit of Fig.1.[2] There are several other 3rd-order circuits [35]-[40] and systems [41]-[43] which are also known to have strange attractors. All of these circuits and systems are described by a continuous, odd-symmetric (with respect to some point of symmetry) piecewise-linear vector field in $\mathcal{R}^3$. While all of these attractors appear to be different from each other, it is natural to ask whether a homeomorphic image of some, if not all, of these attractors might also be found in Chua's circuit with an appropriate choice of the 6 circuit parameters $\{C_1, C_2, L, R, G_a, G_b\}$. In particular, if such a homeomorphism holds globally in the entire state space for all trajectories, the two systems are identical from a dynamical point of view, and the two circuits are therefore said to be *equivalent.* To answer this question, let (μ_1, μ_2, μ_3) denote the eigenvalues associated with the linear vector field in the region D_0 corresponding to the inner segment through the origin (with slope $G_j = G_a$) in Fig.1(b). Let (ν_1, ν_2, ν_3) denote the eigenvalues associated with the affine vector field in the regions D_1 and D_{-1} corresponding to the outer segments (with

[2] In Table 1-5, we have scaled the circuit parameters to a reasonable range for readers who wish to observe the attractors in a real circuit implementation.

identical slope $G_j = G_b$) in Fig.1(b). Let (μ_1', μ_2', μ_3'), and (ν_1', ν_2', ν_3') be the eigenvalues of the corresponding linear and affine vector fields, respectively, of any circuit candidate from Ref.[35]-[40], or system candidate from Ref.[41]-[43]. It follows from *Theorem 3.1* (p.1078) of Ref.[4] that this candidate is *equivalent*, or *topologically conjugate* to be precise [44], to Chua's circuit if, and only if, $\mu_j' = \mu_j$, and $\nu_j' = \nu_j$, $j = 1, 2, 3$. Hence, the following algorithm can be used to find the parameters so that Chua's circuit has an attractor which is homeomorphic to that of a given circuit or system candidate:[3]

Equivalent Chua's Circuit Algorithm

1. Calculate the eigenvalues (μ_1', μ_2', μ_3'), and (ν_1', ν_2', ν_3') associated with the linear and affine vector fields, respectively, of the circuit or system candidate whose *attractor* is being *mapped into* Chua's circuit, up to a homeomorphism (i.e., linear conjugacy).

2. Find a set of circuit parameters $\{C_1, C_2, L, R, G_a, G_b\}$ so that the resulting eigenvalues μ_j, ν_j for Chua's circuit satisfy $\mu_j = \mu_j'$ and $\nu_j = \nu_j'$, $j = 1, 2, 3$.

2.2 *Eigenvalue Constraints in Chua's Circuit*

Unfortunately, in general, the circuit parameters in step 2 do *not* exist for an *arbitrarily* given set of eigenvalues $\{\mu_1', \mu_2', \mu_3'; \nu_1', \nu_2', \nu_3'\}$. To uncover the reason, consider the following characteristic polynomial associated with the Jacobian matrix in regions D_0, and D_1, D_{-1}, respectively:

$$(s - \mu_1)(s - \mu_2)(s - \mu_3) = s^3 - p_1 s^2 + p_2 s - p_3 \quad (1)$$

$$(s - \nu_1)(s - \nu_2)(s - \nu_3) = s^3 - q_1 s^2 + q_2 s - q_3 \quad (2)$$

[3] The proof of Theorem 3.1 in Ref.[4] is given for the case where the circuit has a pair of complex-conjugate eigenvalues in the linear and affine regions. It can be easily shown that the theorem holds also when all 3 eigenvalues are real numbers.

where

$$\left.\begin{array}{ll} p_1 = \mu_1 + \mu_2 + \mu_3 & q_1 = \nu_1 + \nu_2 + \nu_3 \\ p_2 = \mu_1\mu_2 + \mu_2\mu_3 + \mu_3\mu_1 & q_2 = \nu_1\nu_2 + \nu_2\nu_3 + \nu_3\nu_1 \\ p_3 = \mu_1\mu_2\mu_3 & q_3 = \nu_1\nu_2\nu_3 \end{array}\right\} \quad (3)$$

Since the set $\{p_1, p_2, p_3; q_1, q_2, q_3\}$ is *uniquely* determined by the eigenvalues $\{\mu_1, \mu_2, \mu_3; \nu_1, \nu_2, \nu_3\}$ via Eq.(3), we will henceforth refer to it as the "equivalent eigenvalue parameters." These parameters are more convenient to work with in practice not only because they are just the coefficients of the characteristic polynominals (1) and (2), thereby simplifying the subsequent algebra in deriving the circuit parameters, but also because they are *real* numbers, whereas the associated eigenvalues may be complex numbers. Now it is shown in Ref.[45] that there exists a set of circuit parameters $\{C_1, C_2, L, R, G_a, G_b\}$ in step 2 of the Equivalent Chua's Circuit Algorithm *only if* the equivalent eigenvalue parameters satisfy the constraint (see Eq.(21) of Ref.[45]):

$$h(p_1, p_2, p_3, q_1, q_2, q_3) \;\triangleq\; (p_2 - q_2)(p_3 - q_3) - (p_1 - q_1)(p_3 q_1 - q_3 p_1) = 0 \qquad (4)$$

Equation (4) defines a 5-dimensional surface in $\mathcal{R}^6$. Only those circuit candidates from Ref.[35]-[40], or system candidates from Ref.[41]-[43], whose equivalent eigenvalue parameters fall on this surface can have an equivalent Chua's circuit. It follows from this analysis that the class of circuits and systems which are equivalent to Chua's circuit is relatively small. This result has led to a search for the *simplest* circuit which is equivalent to all circuits and systems from Ref.[35]-[44], as well as Chua's circuit and others. The first circuit found with this property, except for a set of measure zero, is given in Ref.[45]. Such a circuit is said to be *canonical* because it contains only 7 circuit parameters, which can be shown to be the *minimum* number needed for any circuit satisfying step 2 of the "equivalent Chua's Circuit Algorithm".

3 *Unfolding Chua's Circuit*

Although the circuit in Ref.(45), as well as several other circuits having 7 parameters, which have since been found to be also canonical in the above sense, they are not obtained by augmenting a new circuit element to the circuit of Fig.1 and hence can not be reduced to Chua's circuit by replacing one of the elements by an open or a short circuit. Our main result of this paper is to prove that the circuit shown in Fig.2, obtained by inserting a *linear* resistor R_0 in series with the inductor in Chua's circuit, is also canonical. The state equation for this augmented circuit is given by

$$\boxed{\begin{aligned} \frac{dv_1}{dt} &= \frac{1}{C_1}[G(v_2 - v_1) - f(v_1)] \\ \frac{dv_2}{dt} &= \frac{1}{C_2}[G(v_1 - v_2) + i_3] \\ \frac{di_3}{dt} &= -\frac{1}{L}(v_2 + R_0 i_3) \end{aligned}} \tag{5}$$

where

$$G = \frac{1}{R}$$

and

$$f(v_1) = G_b v_1 + \frac{1}{2}(G_a - G_b)\{|v_1 + E| - |v_1 - E|\} \tag{6}$$

denotes the odd-symmetric $v - i$ characteristic shown in Fig.2(b) of the nonlinear resistor with a slope equal to G_a in the inner region, and G_b in the outer regions. The voltage E is the breakpoint voltage which can be assumed to be equal to unity without any loss of generality in so far as the qualitative dynamics is concerned. On the other hand, the two slopes G_a and G_b may assume *any sign and value.*

Equation (5) is called a *global unfolding* of Chua's circuit because of its analogy to the mathematical theory of the "unfolding of a singularity" of a vector field [44], where a minimum number of parameters is added in order to observe the dynamics near the singular point in its *full generality.* However, in contrast to the normal form theory of unfolding, which is a *local theory* applicable only to a small neighborhood of a singular point, our unfolded equation (5) is defined over the entire state space $\mathcal{R}^3$, and hence it is called a *global* unfolding. Indeed, we will prove in Section 3 that the unfolded Chua's circuit in Fig.2 is *canonical* in the sense that it is imbued with *every possible qualitative dynamics* of an extremely large family C of piecewise-linear differential equations in $\mathcal{R}^3$ to be defined precisely in Section 4. But, first, we will show that the unfolded Chua's circuit in Fig.2 contains enough circuit parameters for it to realize any prescribed set of eigenvalues $\{\mu_1, \mu_2, \mu_3, \nu_1, \nu_2, \nu_3\}$, except for a set of measure zero. Let us calculate the Jacobian matrix $\mathbf{M}_a$ in region D_0 and $\mathbf{M}_b$ in region D_1 and D_{-1}, respectively:

$$\mathbf{M}_j = \begin{bmatrix} -\frac{G+G_j}{C_1} & \frac{G}{C_1} & 0 \\ \frac{G}{C_2} & -\frac{G}{C_2} & \frac{1}{C_2} \\ 0 & -\frac{1}{L} & -\frac{R_0}{L} \end{bmatrix} \tag{7}$$

where $j = a$ in region D_0, and $j = b$ in regions D_1 and D_{-1}. The characteristic polynomial of $\mathbf{M}_j$ is given by:

$$\begin{aligned} \det(s\mathbf{1} - \mathbf{M}_j) &= s^3 + [\frac{G+G_j}{C_1} + \frac{G}{C_2} + \frac{R_0}{L}]s^2 \\ &+ [\frac{GG_j}{C_1C_2} + \frac{G+G_j}{C_1L}R_0 + \frac{GR_0}{C_2L} + \frac{1}{C_2L}]s + \frac{R_0GG_j + G + G_j}{C_1C_2L} \end{aligned}$$

Identifying the coefficients of s^2, s^1, and s^0 in Eqs.(1) and (2) with Eq.(8) where $j = a$ in D_0, and $j = b$ in D_1 and D_{-1}, we obtain:

$$\frac{G+G_a}{C_1} + \frac{G}{C_2} + \frac{R_0}{L} = -p_1 \tag{8}$$

$$\frac{GG_a}{C_1C_2} + \frac{G+G_a}{C_1L}R_0 + \frac{GR_0}{C_2L} + \frac{1}{C_2L} = p_2 \tag{9}$$

$$\frac{R_0GG_a + G + G_a}{C_1C_2L} = -p_3 \tag{10}$$

which hold in the inner region D_0, and

$$\frac{G+G_b}{C_1} + \frac{G}{C_2} + \frac{R_0}{L} = -q_1 \tag{11}$$

$$\frac{GG_b}{C_1C_2} + \frac{G+G_b}{C_1L}R_0 + \frac{GR_0}{C_2L} + \frac{1}{C_2L} = q_2 \tag{12}$$

$$\frac{R_0GG_b + G + G_b}{C_1C_2L} = -q_3 \tag{13}$$

which hold in the outer regions D_1 and D_{-1}.

Equations (9)-(14) constitute a system of 6 independent equations involving 7 *unknown* circuit parameters $\{C_1, C_2, L, R, R_0, G_a, G_b\}$ and 6 *known* (prescribed) equivalent eigenvalue parameters $\{p_1, p_2, p_3, q_1, q_2, q_3\}$. Hence, we can assign a convenient value to one of the circuit parameters and solve for the rest. After some involved algebra, we obtain the following *explicit* formulas:

$$\boxed{\begin{array}{lcl} C_1 & = & 1 \\ C_2 & = & -\frac{k_2}{{k_3}^2} \\ L & = & -\frac{{k_3}^2}{k_4} \\ R & = & -\frac{k_3}{k_2} \\ R_0 & = & -\frac{k_1 {k_3}^2}{k_2 k_4} \\ G_a & = & -p_1 - (\frac{p_2-q_2}{p_1-q_1}) + \frac{k_2}{k_3} \\ G_b & = & -q_1 - (\frac{p_2-q_2}{p_1-q_1}) + \frac{k_2}{k_3} \end{array}} \tag{14}$$

where $\{p_1, p_2, p_3, q_1, q_2, q_3\}$ are the "equivalent eigenvalue parameters" defined in Eq.(3), and

$$\boxed{\begin{array}{lcl} k_1 & \triangleq & -p_3 + (\frac{q_3-p_3}{q_1-p_1})(p_1 + \frac{p_2-q_2}{q_1-p_1}) \\ k_2 & \triangleq & p_2 - (\frac{q_3-p_3}{q_1-p_1}) + (\frac{p_2-q_2}{q_1-p_1})(\frac{p_2-q_2}{q_1-p_1} + p_1) \\ k_3 & \triangleq & (\frac{p_2-q_2}{q_1-p_1}) - \frac{k_1}{k_2} \\ k_4 & \triangleq & -k_1 k_3 + k_2(\frac{p_3-q_3}{p_1-q_1}) \end{array}} \tag{15}$$

It follows from the explicit formulas in Eqs.(15)-(16) that the "unfolded" Chua's circuit in Fig.2 can realize any eigenvalues parameters $\{ p_1, p_2, p_3, q_1, q_2, q_3 \}$, except for a set of *measure zero* $\subset \mathcal{R}^6$ where some denominators in Eqs.15-16 vanish. In particular, any set of eigenvalue parameters satisfying the following constraints has an associated vector field belonging to $\mathcal{E}_0$:

$$\boxed{\begin{array}{lcl} p_1 - q_1 & = & 0 \\ p_2 - (\frac{q_3-p_3}{q_1-p_1}) + (\frac{p_2-q_2}{q_1-p_1})(\frac{p_2-q_2}{q_1-p_1} + p_1) & = & 0 \\ (\frac{p_2-q_2}{q_1-p_1}) - \frac{k_1}{k_2} & = & 0 \\ -k_1 k_3 + k_2(\frac{p_3-q_3}{p_1-q_1}) & = & 0 \end{array}} \tag{16}$$

Observe from Eqs.(15) and (16) that $R_0 = 0$ when $k_1 = 0$, which is exactly Eq.(4). In other words, when the prescribed eigenvalue parameters belong to the original Chua's circuit in Fig.1, the calculated value of R_0 will be zero, as it should.

Since the set of eigenvalue parameters $\subset \mathcal{R}^6$ which can not be realized by the unfolded Chua's circuit in Fig.2 has *measure zero*, we can make an arbitrarily small perturbation of any unrealizable eigenvalues belonging to this set to obtain an unfolded Chua's circuit having the "perturbed" eigenvalues

$$\{\mu_1 + \delta\mu_1, \mu_2 + \delta\mu_2, \mu_3 + \delta\mu_3, \nu_1 + \delta\nu_1, \nu_2 + \delta\nu_2, \nu_3 + \delta\nu_3\} \tag{17}$$

Since the solution of any system of ordinary differential equations [46]

$$\dot{\mathbf{x}} = \mathbf{f}(\mathbf{x};\mathbf{p}), \qquad \mathbf{f}(\cdot) \in C^1 \tag{18}$$

is a *continuous* function of its parameter vector $\mathbf{p}$, it follows that for *every* circuit or system belonging to the family $\mathcal{C}$, we can find an unfolded Chua's circuit which has exactly the same dynamic behaviors.

4 *Topological Conjugacy*

The vector field defined by Eq.(5) is but a special case of a much larger family of vector fields which we define next.

Definition: Family C

A circuit, system, or vector field defined by a state equation

$$\dot{\mathbf{x}} = \mathbf{f}(\mathbf{x}), \qquad \mathbf{x} \in R^3 \tag{19}$$

is said to belong to *Family C* iff

(a) $f(\cdot)$ is continuous

(b) $f(\cdot)$ is odd-symmetric, i.e.,[4]

$$\mathbf{f}(\mathbf{x}) = -\mathbf{f}(-\mathbf{x})$$

(c) $\mathcal{R}^3$ is partitioned by 2 parallel boundary planes U_1 and U_{-1} into an inner region D_0 containing the origin, and two outer regions D_1 and D_{-1}.

[4] we can relax this condition further by allowing the symmetry to be with respect to a point different from the origin, as in the case of Sparrow's system [43].

Although the boundary planes U_1 and U_{-1} can have any orientation, we will, without loss of generality, assume that a set of coordinate systems has been chosen so that U_1 and U_{-1} are defined as follow ($\mathbf{x} = (x_1, x_2, x_3)^T$):

$$U_1 : x_1 \;=\; 1 \tag{20}$$

$$U_{-1} : x_1 \;=\; -1 \tag{21}$$

Under this assumption, every member of the family C can be represented by

$$\dot{\mathbf{x}} \;=\; \mathbf{A}\,\mathbf{x} + \mathbf{b}, \qquad x_1 \geq 1 \text{ or } x_1 \leq -1 \tag{22}$$

$$\;=\; \mathbf{A}_0\,\mathbf{x}, \qquad -1 \leq x_1 \leq 1 \tag{23}$$

where

$$\mathbf{A} \;=\; \begin{bmatrix} a_{11} & a_{12} & a_{13} \\ a_{21} & a_{22} & a_{23} \\ a_{31} & a_{32} & a_{33} \end{bmatrix}, \qquad \mathbf{b} = \begin{bmatrix} b_1 \\ b_2 \\ b_3 \end{bmatrix} \tag{24}$$

defines an *affine* vector field in the outer regions D_1 and D_{-1}, and

$$\mathbf{A}_0 \;=\; \begin{bmatrix} \alpha_{11} & \alpha_{12} & \alpha_{13} \\ \alpha_{21} & \alpha_{22} & \alpha_{23} \\ \alpha_{31} & \alpha_{32} & \alpha_{33} \end{bmatrix} \tag{25}$$

defines a *linear* vector field in the inner region D_0.

Equations (23)-(26) define a 21-parameter family of ordinary differential equations. However, since the vector field in the family C is *continuous*, not all of these 21 parameters can be arbitrarily specified [4]. In fact, by imposing the continuity constraint, it is easy to show that Eq.22 can be recast into the following equivalent but much more compact explicit form [47]:

$$\dot{\mathbf{x}} \;=\; \mathbf{A}\,\mathbf{x} + \frac{1}{2}\{|<\mathbf{w},\mathbf{x}> +1| - |<\mathbf{w},\mathbf{x}> -1|\}\mathbf{b} \tag{26}$$

where $\mathbf{A}$ and $\mathbf{b}$ are as defined in Eq.(23), $\mathbf{w} = (1,0,0)^T$, and $<,>$ denotes the vector dot product. Obsreve that for $|x| \geq 1$, Eq.(27) reduces to Eq.(23). Similarly, when $|x| \leq 1$, Eq.(27) reduces to Eq.(24), upon identifying

$$\mathbf{A}_0 = \mathbf{A} + \begin{bmatrix} b_1 & 0 & 0 \\ b_2 & 0 & 0 \\ b_3 & 0 & 0 \end{bmatrix} \tag{27}$$

In other words, the continuity of the vector fields in the family $\mathcal{C}$ implies that the last two columns of the matrices $\mathbf{A}$ and $\mathbf{A}_0$ must be identical, and that their first columns must differ by the constant vector $\mathbf{b}$. It follows from Eq.(28) that the family $\mathcal{C}$ of vector fields represents in fact a 12-parameter familty of ordinary differential equations *without constraints* among the parameters, or a 21-parameter family where 9 of the 21 parameters $\{a_{ij}, \alpha_{ij}, b_i; i, j = 1, 2, 3\}$ are constrained via Eq.(28).

Since we have given the *explicit* formulas (Eqs.(15)-(16)) for calculating the 7 circuit parameters for the unfolded Chua's circuit in Fig.2 to have any *prescribed* eigenvalues, except for a set of measure zero, we can conclude via *Theorem 3.1* from Ref.[4] that every member of the family $\mathcal{C}$ of vector fields outside of the set $\mathcal{E}_0$ (to be defined shortly) is topologically conjugate to an unfolded Chua's circuit. The proof of Theorem 3.1 in Ref.[4] assumes that both $\mathbf{A}_0$ and $\mathbf{A}$ have a pair of complex-conjugate eigenvalues because it was intended mainly for the double scroll attractor. A similar proof can be easily given when the eigenvalues of $\mathbf{A}_0$ and/or $\mathbf{A}$ are all real numbers. We will now restate this fundmental theorem precisely and give a self-contained and simpler proof.

The Global Unfolding Theorem

Let $\{ \mu_1, \mu_2, \mu_3, \nu_1, \nu_2, \nu_3 \}$ be the eigenvalues associated with a vector field $\mathbf{F}(\mathbf{x}) \in \mathcal{C} \setminus \mathcal{E}_0$, where $\mathcal{E}_0$ is a set of vector fields whose eigenvalue parameters are constrained by Eq. (17), and by det $\mathbf{K} = 0$, where $\mathbf{K}$ is defined by the following Eq.(30). Then the unfolded Chua's circuit with parameters defined by Eqs.(15)-(16) is *linearly-conjugate*, and hence *equivalent*, to this vector field.

Proof. Without loss of generality, assume that $\mathbf{F}(\mathbf{x})$ is defined by Eq.(27), with $\mathbf{A}$ and $\mathbf{b}$ defined by Eq.(25). Define the non-singular transformation

$$\mathbf{y} \;=\; \mathbf{K}\,\mathbf{x} \tag{28}$$

where

$$\mathbf{K} \;=\; \begin{bmatrix} 1 & 0 & 0 \\ a_{11} & a_{12} & a_{13} \\ K_{31} & K_{32} & K_{33} \end{bmatrix} \tag{29}$$

(30)

and

$$K_{3i} \;\triangleq\; \sum_{j=1}^{3} a_{1j}a_{ji}, \qquad i = 1,2,3 \tag{31}$$

Since $\mathbf{F}(\mathbf{x}) \notin \mathcal{E}_0$,

$$\det \mathbf{K} \;=\; a_{12}K_{33} - a_{13}K_{32} \neq 0 \tag{32}$$

Hence, $\mathbf{K}^{-1}$ exists and Eq.(27) transforms into

$$\dot{\mathbf{y}} \;=\; (\mathbf{KAK}^{-1})\mathbf{y} + \frac{1}{2}\{|<(\mathbf{K}^{-1})^T\mathbf{w},\mathbf{y}>+1| - |<(\mathbf{K}^{-1})^T\mathbf{w},\mathbf{y}>-1|\}\mathbf{Kb} \tag{33}$$

where

$$\mathbf{KAK}^{-1} \;=\; \begin{bmatrix} 0 & 1 & 0 \\ 0 & 0 & 1 \\ p_3 & -p_2 & p_1 \end{bmatrix} \triangleq \hat{\mathbf{A}} \tag{34}$$

is the *companion* matrix of $\mathbf{A}$,

$$(\mathbf{K}^{-1})^T\mathbf{w} = \begin{bmatrix} 1 \\ 0 \\ 0 \end{bmatrix} \triangleq \hat{\mathbf{w}} = \mathbf{w} \tag{35}$$

$$\mathbf{Kb} = \begin{bmatrix} p_1 - q_1 \\ -p_2 + q_2 + q_1(p_1 - q_1) \\ p_3 - q_3 - q_2(p_1 - q_1) + q_1[-p_2 + q_2 + q_1(p_1 - q_1)] \end{bmatrix} \triangleq \hat{\mathbf{b}} \tag{36}$$

Hence, the transformed vector field simplifies to

$$\dot{\mathbf{y}} = \hat{\mathbf{A}}\mathbf{y} + \frac{1}{2}\{| < \mathbf{w}, \mathbf{y} > +1| - | < \mathbf{w}, \mathbf{y} > -1|\}\hat{\mathbf{b}} \tag{37}$$

henceforth called the *companion vector field.* Observe that both $\hat{\mathbf{A}}$ and $\mathbf{b}$ are *uniquely* determined by the prescribed eigenvalues $\{ \mu_1, \mu_2, \mu_3, \nu_1, \nu_2, \nu_3 \}$ via their equivalent eigenvalue parameters

$$\{p_1,\ p_2,\ p_3,\ q_1,\ q_2,\ q_3\} \tag{38}$$

We have therefore shown that the given vector field $\mathbf{F}(\mathbf{x})$ is topologically conjugate to the companion vector field $\hat{\mathbf{F}}(\mathbf{y})$ defined by Eq.(38).

Now $\mathbf{F}(\mathbf{x}) \in \mathcal{C} \setminus \mathcal{E}_0$ implies that there exists an unfolded Chua's circuit defined by the vector field $\tilde{\mathbf{f}}(\tilde{\mathbf{x}})$ with $\tilde{\mathbf{x}} = (v_1, v_2, i_3)^T$ via Eq.(5) that has *the* same prescribed set of eigenvalues as those of $\mathbf{F}(\mathbf{x})$. We can recast Eq.(5), with $E = 1$, into the canonical piecewise-linear form

$$\dot{\tilde{\mathbf{x}}} = \tilde{\mathbf{A}}\tilde{\mathbf{x}} + \frac{1}{2}\{| < \mathbf{w}, \tilde{\mathbf{x}} > +1| - | < \mathbf{w}, \tilde{\mathbf{x}} > -1|\}\tilde{\mathbf{b}} \tag{39}$$

where

$$\mathbf{w} = (1, 0, 0)^T \tag{40}$$

$$\tilde{\mathbf{A}} = \begin{bmatrix} -(\frac{G+G_b}{C_1}) & \frac{G}{C_1} & 0 \\ \frac{G}{C_2} & -\frac{G}{C_2} & \frac{1}{C_2} \\ 0 & -\frac{1}{L} & -\frac{R_0}{L} \end{bmatrix}, \qquad \tilde{\mathbf{b}} = \begin{bmatrix} G_a - G_b \\ 0 \\ 0 \end{bmatrix} \tag{41}$$

There exists a corresponding non-singular linear transformation

$$\tilde{\mathbf{y}} = \tilde{\mathbf{K}}\tilde{\mathbf{x}} \tag{42}$$

which transforms Eq.(40) into its corresponding companion vector field by Eq.(38), with $\mathbf{y}$ replaced by $\tilde{\mathbf{y}}$, where

$$\tilde{\mathbf{K}} = \begin{bmatrix} 1 & 0 & 0 \\ -(\frac{G+G_b}{C_1}) & \frac{G}{C_1} & 0 \\ \tilde{K}_{31} & \tilde{K}_{32} & \tilde{K}_{33} \end{bmatrix} \tag{43}$$

and

$$\tilde{K}_{31} = \tilde{a}_{11}\tilde{a}_{11} + \tilde{a}_{12}\tilde{a}_{21} + \tilde{a}_{13}\tilde{a}_{31} = (\frac{G+G_b}{C_1})^2 + \frac{G^2}{C_1C_2} \tag{44}$$

$$\tilde{K}_{32} = \tilde{a}_{11}\tilde{a}_{12} + \tilde{a}_{12}\tilde{a}_{22} + \tilde{a}_{13}\tilde{a}_{32} = -\frac{G(G+G_b)}{{C_1}^2} - \frac{G^2}{C_1C_2} \tag{45}$$

$$\tilde{K}_{33} = \tilde{a}_{11}\tilde{a}_{13} + \tilde{a}_{12}\tilde{a}_{23} + \tilde{a}_{13}\tilde{a}_{33} = \frac{G}{C_1C_2} \tag{46}$$

But since $\tilde{\mathbf{A}}$ and $\tilde{\mathbf{b}}$ in Eq.(42) are determined *uniquely* by *only* the equivalent eigenvalue parameters $\{p_1, p_2, p_3, q_1, q_2, q_3\}$, it follows that both $\mathbf{F}(\mathbf{x})$ and $\tilde{\mathbf{f}}(\mathbf{x})$ must transform into one and the *same* companion vector field. Hence, we have $\mathbf{y} = \tilde{\mathbf{y}}$. It follows from Eqs.(29) and (43) that

$$\mathbf{x} = \mathbf{T}\begin{bmatrix} v_1 \\ v_2 \\ i_3 \end{bmatrix} \tag{47}$$

where

$$\mathbf{T} \triangleq \mathbf{K}^{-1}\tilde{\mathbf{K}} \tag{48}$$

transforms every circuit, system, or vector field belonging to the family $\mathcal{C} \setminus \mathcal{E}_0$ into an unfolded Chua's circuit. This completes the proof of our main theorem. □

Remarks:

1. The unfolded Chua's circuit in the global unfolding theorem is *unique*, modulo a normalization constant C_1, which was assumed to be unity in Eq.(15(a)) for convenience. Using the language from *linear* circuit theory, this normalization corresponds to setting the "impedance level" of the linearized small-signal equivalent circuit.

2. Any unrealizable vector field belonging to the set $\mathcal{E}_0$ can be perturbed to a *qualitatively* identical vector field belonging to the family $\mathcal{C}$, and hence once again realizable by an unfolded Chua's circuit. In practice, to avoid numerical ill conditioning, it is more convenient to perturb the equivalent eigenvalue parameters from $\{p_1, p_2, p_3, q_1, q_2, q_3\}$ into $\{p_1 + \delta p_1, p_2 + \delta p_2, p_3 + \delta p_3, q_1 + \delta q_1, q_2 + \delta q_2, q_3 + \delta q_3\}$, where δp_i and δq_i are chosen to be sufficiently small (at least one must be non-zero).

3. The condition given in Eq.(33) is equivalent to the assumption that there is no plane or line parallel to the boundary planes which is invariant under the action of the linear vector field in the middle region.

5 *Applications of the Unfolded Canonical Chua's Circuit*

5.1 *Mapping Chaotic Circuits from Family $\mathcal{C}$*

We can now easily "map" any chaotic circuit belonging to the family of vector fields $\mathcal{C} \setminus \mathcal{E}_0$ into the unfolded canonical Chua's circuit shown in Fig.2 by applying *Step1* of the *Equivalent Chua's Circuit Algorithm* from Section 2.1 and calculating the circuit parameters $\{C_1, C_2, L, R, R_0, G_a, G_b\}$ using Eqs.(15)-(16).

The purpose of this section is to illustrate this procedure by selecting a few chaotic circuits belonging to $\mathcal{C} \setminus \mathcal{E}_0$ and demonstrate the immense advantage of this unifying approach via a single circuit of universal utility.

Esample 1. Consider the chaotic circuit given in Fig.1 of Ref.[38], and its strange attractor in Fig.3 which we reproduce below in Fig.3(a). Using the circuit parameters provided in Ref.[38], we have calculated the following eigenvalues:

$$\left.\begin{array}{lll} \mu_1 = 0.367929, & \mu_2 = -0.283965 + j1.1306, & \mu_3 = -0.283965 - j1.1306 \\ \nu_1 = -10.9656, & \nu_2 = 0.132777 + j0.945683, & \nu_3 = 0.132777 - j0.945683 \end{array}\right\} \tag{49}$$

The corresponding equivalent eigenvalue parameters calculated from Eq.(3) are given by:

$$\left.\begin{array}{lll} p_1 = -0.188575, & p_2 = -1.406646, & p_3 = -0.04406605 \\ q_1 = -10.699046, & q_2 = -3.7886455, & q_3 = 9.6133946 \end{array}\right\} \tag{50}$$

Substituting the parameters from Eq.(51) into Eqs.(15)-(16), we obtain the following parameters for the equivalent "unfolded" canonical Chua's circuit:

$$\left.\begin{array}{lll} C_1 = 1, & C_2 = -0.0326059, & L = -2.760292 \\ R = -10.11087, & G = -0.098903457, & R_0 = 9.200877, \\ G_a = 0.5989046, & G_b = 11.09895 & \end{array}\right\} \tag{51}$$

The strange attractor associated with Eq.(52) is shown in Fig.3(b). While the 2 attractors in Fig.3 are not identical to each other, they are in fact equivalent in view of the *global unfolded theorem* from the preceding section. In fact, they are related by the transformation matrix $\mathbf{T} = \mathbf{K}^{-1}\tilde{\mathbf{K}}$ in Eq.(49), where

$$\mathbf{K} = \begin{bmatrix} 1 & 0 & 0 \\ -\frac{b}{\epsilon} & 0 & -b \\ \frac{b^2}{\epsilon^2} + \frac{b^2}{\epsilon} & b & \frac{b^2}{\epsilon} - b(a-b) \end{bmatrix} = \begin{bmatrix} 1 & 0 & 0 \\ -10 & 0 & -1 \\ 110 & 1 & 10.7 \end{bmatrix} \tag{52}$$

and

$$\tilde{\mathbf{K}} = \begin{bmatrix} 1 & 0 & 0 \\ -11.000047 & -0.0989035 & 0 \\ 120.7010302 & 1.387946472 & 3.033299403 \end{bmatrix} \tag{53}$$

where ε, a, and b are parameters from Ref.[38].

To verify that the 2 strange attractors in Fig.3 are in fact one and *the same* attractor expressed in different coordinate systems, we multiply the coordinates $(\tilde{x}_1, \tilde{x}_2, \tilde{x}_3) = (v_1, v_2, i_3)$ of the time series of the attractor in Fig.3(b) from the canonical Chua's circuit by the matrix $\mathbf{T}$, and obtain the attractor shown in Fig.3(a), as expected.

Example 2. Period-Doubling Route to Chaos

Table 2 shows the waveform and spectrum of $v_1(t)$ and its associated attractor obtained from previous publications on Chua's circuit. Table 2.1 shows a pair of periodic orbits which bifurcated from two stable equlibrium points $P^+ \in D_1$ and $P^- \in D_{-1}$, via Hopf bifurcation. As we vary a single parameter C_1 from $C_1 = 11.364\,\mathrm{nF}$ down to $C_1 = 10.204\,\mathrm{nF}$, while keeping all other parameters fixed, we obtain the well-known *period-doubling route* to chaos, as shown in Tables 2.2 (period 2), 2.3 (period 4), 2.4 (period 8), 2.5 (Rössler attractor), and 2.6 (Double Scroll Attractor). If we substitute the eigenvalues associated with each attractor in Table 2 into Eqs.(15)-(16), we would obtain the corresponding parameters indicated in this table (scaled by a factor to obtain reasonable circuit parameters). Notice that $R_0 = 0$ in each case, as expected.

Example 3. Intermittency Route to Chaos

Table 3 shows the waveform and spectrum of $v_1(t)$ and its associated attractor obtained by mapping corresponding attractors from the earlier canonical Chua's circuit in Ref.[45]. Using the eigenvalues calculated from Eq.(3) in Ref.[45] for the attractors shown in Figs.3 (a),(b),(c),(d), and (e) of Ref.[45], we obtain the corresponding attractors using the unfolded canonical Chua's circuit, as shown in Table 3.1, 3.2, 3.3, 3.5, and 3.6. Note that while some of these attractors may not look very similar to their corresponding attractor in Fig.3 of Ref.(45), they are in fact related by the transformation matrix **T** defined in Eq.(49). Table 3.4 provides another attractor not given in Ref.[45] but which illustrates the evolution of the intermittency phenomenon in greater detail.

Example 4. Torus Breakdown Route to Chaos

Table 4 shows the waveform and spectrum of $v_1(t)$ and its associated attractor obtained by mapping corresponding attractors from the *torus circuit* given in Ref.[35].[5] Using the eigenvalues calculated from Eq.(1) of Ref.[35] for the attractors shown in Fig.5 of Ref.[35], we found these eigenvalues belong to the set of unrealizable eigenvalues (as defined by Eq. (17)). Using the slightly perturbed eigenvalues shown in Table 4 (scaled to obtain reasonable parameter values), we obtain the corresponding attractors shown in Tables 4.1-4.6.

5.2 *Mapping Chaotic Systems from Family C*

Consider the chaotic feedback system given by Brockett in Ref.[42], and its strange attractor given in Fig.9 (page 936), which we reproduce in Fig.4(a). Using the system parameters provided in Ref.[42], we have calculated the following eigenvalues:

$$\left.\begin{array}{lll} \mu_1 = 0.721965, & \mu_2 = -0.860982 + j1.3236, & \mu_3 = -0.860982 - j1.3236 \\ \nu_1 = -1.61109, & \nu_2 = 0.305544 + j1.46327, & \nu_3 = 0.305544 - j1.46327 \end{array}\right\} \tag{54}$$

The corresponding equivalent eigenvalue parameters calculated from Eq.(3) are given by:

$$\left.\begin{array}{lll} p_1 = -1, & p_2 = 1.25, & p_3 = 1.8 \\ q_1 = -1, & q_2 = 1.25, & q_3 = -3.6 \end{array}\right\} \tag{55}$$

Observe that $p_1 = q_1$ and hence Brockett's system also belongs to the set $\mathcal{E}_0$. To obtain a qualitatively similar strange attractor using the unfolded canonical Chua's circuit from Fig.2, we add a small perturbation δp_1 = 0.05 and δq_1 = -0.05 to obtain

$$\left.\begin{array}{lll} p_1{}' = -0.95, & p_2{}' = 1.25, & p_3{}' = 1.8 \\ q_1{}' = -1.05, & q_2{}' = 1.25, & q_3{}' = -3.6 \end{array}\right\} \tag{56}$$

[5]This circuit was discovered and studied extensively by R. Tokunaga.

These equivalent eigenvalue parameters corresponds to the following set of perturbed eigenvalues

$$\left.\begin{array}{lll} \mu_1{}' = 0.728163, & \mu_2{}' = -0.839081 + j1.3296, & \mu_3{}' = -0.839081 - j1.3296 \\ \nu_1{}' = -1.6337, & \nu_2{}' = -0.2918491 + j1.45548, & \nu_3{}' = -0.2918491 - j1.45548 \end{array}\right\} \quad (57)$$

Substituting Eq.(52) into Eqs.(15)-(16), we obtain the following parameters for the equivalent "unfolded" canonical Chua's circuit:

$$\left.\begin{array}{rll} C_1 = 1, & C_2 = 54.08314, & L = 0.0003490195 \\ R = -0.01907856, & R_0 = 0.0003512879, & \\ G_a = 53.36472, & G_b = 53.46473 & \end{array}\right\} \quad (58)$$

The strange attractor associated with the parameters in Eq.(59) is shown in Fig.4(b). Again, to map Fig.4(b) into Fig.4(a), we calculate the transformation matrix $\mathbf{T} = \mathbf{K}^{-1}\tilde{\mathbf{K}}$ in Eq.(49), where

$$\mathbf{K} = \begin{bmatrix} 1 & 0 & 0 \\ 0 & 1 & 0 \\ 0 & 0 & 1 \end{bmatrix} \quad (59)$$

and

$$\tilde{\mathbf{K}} = \begin{bmatrix} 1 & 0 & 0 \\ -1.049873 & -52.414857 & 0 \\ 51.90026889 & 4.230907969 & -0.956509787 \end{bmatrix} \quad (60)$$

Multiplying the coordinates $(\tilde{x}_1, \tilde{x}_2, \tilde{x}_3) = (v_1, v_2, i_3)$ of the time series of the attractor in Fig.4(b) from the canonical Chua's circuit by the matrix $\mathbf{T}$, we obtain an attractor which is *qualitatively similar* to that of Fig.4(a), as expected.

5.3 *A Zoo of Strange Attractors from Family C*

More than 30 non-periodic attractors from the family C of vector fields have been observed from many 3rd-order electronic circuits and systems, and from computer simulations. Table 5 shows a sample of some of these attractors which have been mapped into the unfolded canonical Chua's circuit of Fig.2. Many of these attractors mapped are from those presented in Ref.[45]. For example, Tables 5.1, 5.2, 5.3, 5.4, 5.5, 5.7, 5.10, 5.12, 5.13 correspond to the attractors given in Figs. 19, 18, 20, 8, 9, 12, 14, 7 in Ref.[45] respectively. A gallery of 18 multi-color strange attractors from this table and table 1 (projected into the $v_1 - v_2$ plane) is shown in Table 6.

6 *Concluding Remarks*

All waveforms and attractors in this paper are calculated *numerically* using the user-friendly software package INSITE [48]. Since the circuit parameters for all attractors in Table 1–5 are given, and scaled to within therange of practical component values, *experimental* observations of these attractors can be made by building the unfolded Chua's Circuit with the corresponding circuit parameters. Those parameters which are negative can be realized with the help of a *negative impedance converter* (NIC) having a large enough linear dynamic range. The $v_R - i_R$ characteristic of the nonlinear resistor (Chua's Diode [21]) can be realized by various nonlinear circuit synthesis techniques, such as those given in [49 - 52].

The circuit presented in Fig.2 of this paper, as well as that given in Fig.4 of Ref.(45) are both *canonical* and equivalent to each other. It is interesting to observe that these two circuits can be interpreted as a *global unfolding* of the 2 *chaotic* circuit candidates (Figs.4(g) and (h), p.252) which have been derived by a systematic nonlinear circuit synthesis procedure, as described in Ref.[1]. Both unfoldings are obtained by adding a *linear* resistor in series with the inductor. In fact, many other canonical circuits can also be derived by connecting a linear resistor, by a plier or soldering-iron entry with other elements in these 2 circuits. Since all of these canonical circuits are equivalent to each other, *only one* circuit need to be studied in depth, at least from a theoretical point of view. Since many papers have already been published on Chua's circuit (Fig.1), the unfolded Chua's circuit in Fig.2 will be the circuit of choice in our future research on nonlinear *dynamics* of this circuit. Such a research program is important because any future result or breakthrough applies to the entire family C of 21-

parameter family of vector fields, including all of the chaotic circuits from Refs.[35]-[40], and chaotic systems from Refs.[41]-[43]. In fact, it is natural for us to allow the scalar nonlinear function in Fig.2 to be *any* piecewise continuous function (e.g., polynomial, signum function, etc.) which need not be piecewise-linear or symmetric. We conjecture that most autonomous 3*rd*-order chaotic circuits and systems with polynomial, signum, and hysteretic nonlinearities can be accurately modeled by the above generalization. It is the *universality* and *unifying* potentials of the unfolded canonical Chua's circuit that has made it a fundamental and general tool for understanding and applying *chaotic dynamics* for future applications in science and technology.

7 *Chronological Bibliography*

Since the study of chaotic circuits and systems belonging to the 21-parameter family C of vector fields reduces to the study of the unfolded Chua's circuit of Fig.2, the following bibliography is included, in chronological order for future researchers of this circuit.

T. Matsumoto. A chaotic attractor from Chua's circuit. *IEEE Transactions on Circuits and Systems*, CAS-31(12):1055–1058, 1984.

G. Q. Zhong and F. Ayrom. Experimental confirmation of chaos from Chua's circuit. *International Journal of Circuit Theory and Applications*, 13(11):93–98, 1985.

G. Q. Zhong and F. Ayrom. Periodicity and chaos in Chua's circuit. *IEEE Transactions on Circuits and Systems*, CAS-32(5):501–503, 1985.

T. Matsumoto, L. O. Chua, and M. Komuro. The Double Scroll. *IEEE Transactions on Circuits and Systems*, CAS-32(8):797–818, 1985.

T. Matsumoto, L. O. Chua, and M. Komuro. The Double Scroll bifurcations. *International Journal of Circuit Theory and Applications*, 14(1):117–146, 1986.

T. Matsumoto, L. O. Chua, and K. Tokumasu. Double Scroll via a two-transistor circuit. *IEEE Transactions on Circuits and Systems*, CAS-33(8):828–835, 1986.

F. Ayrom and G. Q. Zhong. Chaos in Chua's circuit. *IEE Proceedings*, 133(6):307–312, 1986.

L. O. Chua, M. Komuro, and T. Matsumoto. The Double Scroll family, parts I and II. *IEEE Transactions on Circuits and Systems*, CAS-33(11):1073–1118, 1986.

C. Kahlert and L. O. Chua. Transfer maps and return maps for piecewise-linear and three-region dynamical systems. *International Journal of Circuit Theory and Applications*, 15(1):23–49, 1987.

T. Matsumoto, L. O. Chua, and M. Komuro. Birth and death of the Double Scroll. *Physica*, 24D:97–124, 1987.

M. J. Ogorzałek. Chaotic regions from Double Scroll. *IEEE Transactions on Circuits and Systems*, CAS-34(2):201–203, 1987.

M. E. Broucke. One-parameter bifurcation diagram for Chua's circuit. *IEEE Transactions on Circuits and Systems*, CAS-34(3):208–209, 1987.

L. Yang and Y. L. Liao. Self-similar structures from Chua's circuit. *International Journal of Circuit Theory and Applications*, 15(2):189–192, 1987.

T. Matsumoto, L. O. Chua, and R. Tokunaga. Chaos via torus breakdown. *IEEE Transactions on Circuits and Systems*, CAS-34(3):240–253, 1987.

S. Wu. Chua's circuit family. *Proceedings of the IEEE*, 75(8):1022–1032, 1987.

T. S. Parker and L. O. Chua. The dual Double Scroll equation. *IEEE Transactions on Circuits and Systems*, CAS-34(9):1059–1073, 1987.

A. I. Mees and P. B. Chapman. Homoclinic and heteroclinic orbits in the Double Scroll attractor. *IEEE Transactions on Circuits and Systems*, CAS-34(9):1115–1120, 1987.

C. Kahlert. The range of transfer and return maps in three-region piecewise-linear dynamical systems. *International Journal of Circuit Theory and Applications*, 16(1):11–23, 1988.

C. Kahlert. Dynamics of the inclusions appearing in the return maps of Chua's circuit - 1. the creation mechanism. *International Journal of Circuit Theory and Applications*, 16(1):29–46, 1988.

M. Komuro. Normal forms of continuous piecewise-linear vector field and chaotic attractors: Part I. *Japan J. Appl. Math*, 5(2):257–304, 1988.

M. Komuro. Normal forms of continuous piecewise-linear vector field and chaotic attractors: Part II. *Japan J. Appl. Math*, 5(3):503–549, 1988.

C. Kahlert. The chaos producing mechanism in Chua's circuit. *International Journal of Circuit Theory and Applications*, 16(2):227–232, 1988.

T. Matsumoto, L. O. Chua, and K. Ayaki. Reality of chaos in the Double Scroll circuit: A computer-assisted proof. *IEEE Transactions on Circuits and Systems*, CAS-35(7):909–925, 1988.

C. P. Silva and L. O. Chua. The overdamped Double Scroll family. *International Journal of Circuit Theory and Applications*, 16(3):233–302, 1988.

P. Bartissol and L. O. Chua. The Double Hook. *IEEE Transactions on Circuits and Systems*, CAS-35(12):1512–1522, 1988.

A. Huang. A study of the chaotic phenomena in Chua's circuit. In *Proceedings of the ISCAS*, pages 273–276, Helsinki, 1988.

R. Tokunaga, T. Matsumoto, M. Komuro, L. O. Chua, and K. Miya. Homoclinic linkage: A new bifurcation mechanism. *Proceedings IEEE ISCAS*, 2:826–829, 1989.

R. Tokunaga, T. Matsumoto, T. Ida, and K. Miya. Homoclinic linkage in the Double Scroll circuit and the cusp-constrained circuit. In N. Aoki, editor, *The Study of Dynamical Systems*, pages 192–209. World Scientific, Singapore, 1989.

L. O. Chua and G. N. Lin. Intermittency in a piecewise-linear circuit. *IEEE Transactions on Circuits and Systems*, CAS-38(5):510–520, 1990.

C. M. Blazquez and E. Tuma. Dynamics of the Double Scroll circuit. *IEEE Transactions on Circuits and Systems*, CAS-37(5):589–593, 1990.

L. O. Chua and G. N. Lin. Canonical realization of Chua's circuit family. *IEEE Transactions on Circuits and Systems*, CAS-37(7):885–902, 1990.

V. Spany and L. Pivka. Boundary surfaces in sequential circuits. *International Journal of Circuit Theory and Applications*, 18(4):349–360, 1990.

M. Komuro. Bifurcation equations of 3-dimensional piecewise-linear vector fields. In H. Kawakami, editor, *Bifurcation Phenomena in Nonlinear Systems and Theory of Dynamical Systems*, pages 113–123. World Scientific, Singapore, 1990.

R. Lozi and S. Ushiki. Co-existing chaotic attractors in Chua's circuit. *International Journal of Bifurcation and Chaos*, 1(4), 1990. in press.

R. Lozi and S. Ushiki. Confinors and bounded-time patterns in Chua's circuit and the Double Scroll family. *International Journal of Bifurcation and Chaos*, 1(1):119–138, 1991.

M. Komuro, R. Tokunaga, T. Matsumoto, and A. Hotta. Global bifurcation analysis of the Double Scroll circuit. *International Journal of Bifurcation and Chaos*, 1(1):139–182, 1991.

L. O. Chua and I. Tichonicky. 1-d map for the double scroll family. *IEEE transactions on circuits and systems*, CAS-38:233–243, March 1991.

K. Murali and M. Lakshmanan. Bifurcation and chaos of the sinusoidally-driven Chua's circuit. *International Journal of Bifurcation and Chaos*, 1(2):369–384, 1991.

C. Kahlert. Heteroclinic orbits and scaled similar structures in the parameter space of the Chua oscillator. In G. Baier and M. Klein, editors, *Chaotic Hierarchy*, pages 209–234. World Scientific, Singapore, 1991.

D. S. Dabby. The buffalo horn and strange behavior in third order autonomous circuits. Master's thesis, Massachusetts Institute of Technology, Electrical Engineering and Computer Science, 1991. 142 pages.

J. Cruz and L. O. Chua. A CMOS IC nonlinear resistor for Chua's circuit. Memorandum, Electronics Research Laboratory, University of California, Berkeley, 1992.

R. Genesio and A. Tesi. Harmonic balance approach for chaos prediction: the Chua's circuit. *International Journal of Bifurcation and Chaos*, 2(1), 1992. in press.

M.P. Kennedy. Robust op amp realization of chua's circuit. *Frequenz*, 46(3-4):66–80, 1992.

V.S. Anishchenko, M.A. Safonova, and L.O. Chua. Stochastic resonance in Chua's circuit. *Int. J. of Bifurcation and Chaos*, 2(2):397–401, June 1992.

V. Perez-Munuzuri, V. Perez-Villar, and L.O. Chua. Propagation failure in linear arrays of Chua's circuits. *Int. J. of Bifurcation and Chaos*, 2(2):403–406, June 1992.

V.N. Belykh and L.O. Chua. New type of strange attractor from a geometric model of Chua's circuit. *Int. J. of Bifurcation and Chaos*, 2(3):697–704, Sept 1992.

Leon O. Chua, Lj. Kocarev, K. Eckert, and M. Itoh. Experimental synchronization in Chua's circuit. *Int. J. of Bifurcation and Chaos*, 2(3):705–708, Sept 1992.

Lj. Kocarev, K. S. Halle, K. Eckert, L.O. Chua, and U. Parlitz. Experimental demonstration of secure communications via chaotic synchronization. *Int. J. of Bifurcation and Chaos*, 2(3), Sept 1992. 709-713.

K. Murali and M. Lakshmanan. Transition from quasiperiodicity to chaos and devil's staircase structures of the driven Chua's circuit. *Int. Journal of Bifurcation and Chaos*, 2(3):621–632, 1992.

A. Dabrowski, Z. Galias and M. J. Ogorzalek. A study of identification and control in a real implementation of Chua's circuit. In *Proc. 2nd IFAC Workship on System Structure and Control, 3-5 September 1992, Prague, Czechoslovakia* (invited papter), pages 278–281.

U. Parlitz, L.O. Chua, Lj. Kocarev, K.S. Halle, and A. Shang. Transmission of digital signals by chaotic synchronization. *Int. J. of Bifurcation and Chaos*, 2(4), Dec 1992. in press.

R. Madan (Guest Editor). *Special Issue on Chua's Circuit: A Paradigm for Chaos, Part I*, volume 1 of *Journal of Circuit, Systems, and Computers*. 1993. (To appear in march 1993).

R. Madan (Guest Editor). *Special Issue on Chua's Circuit: A Paradigm for Chaos, Part II*, volume 2 of *Journal of Circuit, Systems, and Computers*. 1993. (To appear in june 1993).

Acknowledgement

I would like to thank Chai Wah Wu, Ljupco Kocarev and Anshan Huang for their assistance in the preparation of this manuscript.

References

[1] L.O.Chua. The genesis of Chua's circuit. *Archiv fur Elektronik und Ubertragungstechnik*, 46(4):250–257, 1992.

[2] T.Matsumoto. A chaotic attractor from Chua's circuit. *IEEE Trans CAS*, 31(12):1055–1058, 1984.

[3] G.Q. Zhong and F. Ayrom. Experimental confirmation of chaos from Chua's circuit. *Int.J. of Circuit Theory and Applications*, 13(1):93–98, 1985.

[4] L.O.Chua, M.Komuro, and T.Matsumoto. The double scroll family, parts I and II. *IEEE Trans CAS*, 33(11):1073–1118, 1986.

[5] R. N. Madan(Session Organizer). Special session on Chua's circuit:. *Proc. of the 35th Midwest Symposium on Circuits and Systems*, Washington DC., August 1992.

[6] R. N. Madan(Editor). Special issue on Chua's circuit: A paradigm for chaos. *J. of Circuits, Systems, and Computers*, 3(1), March 1993. in press.

[7] R. N. Madan(Editor). Special issue on Chua's circuit: A paradigm for chaos. *J. of Circuits, Systems, and Computers*, 3(2), June 1993. in press.

[8] Leon O. Chua, Lj. Kocarev, K. Eckert, and M. Itoh. Experimental synchronization in Chua's circuit. *Int. J. of Bifurcation and Chaos*, 2(3):705–708, Sep 1992.

[9] Leon O. Chua, M. Itoh, Lj. Kocarev, and K. Eckert. Chaos synchronization in Chua's circuit. *J. of Circuits, Systems, Computers*, 3(1), March 1993. in press.

[10] G. A. Johnson, T. E. Tigner, and E. R. Hunt. Controlling chaos in Chua's circuit. *J. of Circuits, Systems, Computers*, 3(1), March 1993. in press.

[11] G. A. Johnson and E. R. Hunt. Maintaining stability in Chua's circuit driven into regions of oscillation and chaos. *J. of Circuits, Systems and Computers*, 3(1), March 1993. in press.

[12] K. Murali and M. Lakshmanan. Controlling chaos in Chua's circuit. *J. of Circuits, Systems and Computers*, 3(1), March 1993. in press.

[13] G.R. Chen and Dong X.N. Controlling Chua's circuit. *J. of Circuits, Systems and Computers*, 3(1), March 1993. in press.

[14] R. Genesio and A. Tesi. Distortion control of chaotic systems. *J. of Circuits, Systems and Computers*, 3(1), March 1992. 61–79.

[15] T. Hartley and F. Mossayebi. Control of Chua's circuit. *J. of Circuits, Systems and Computers*, 3(1), March 1993. in press.

[16] Lj. Kocarev, K. S. Halle, K. Eckert, L.O. Chua, and U. Parlitz. Experimental demonstration of secure communications via chaotic synchronization. *Int. J. of Bifurcation and Chaos*, 2(4), Dec 1992. 709-713.

[17] U. Parlitz, L.O. Chua, Lj. Kocarev, K.S. Halle, and A. Shang. Transmission of digital signals by chaotic synchronization. *Int. J. of Bifurcation and Chaos*, 2(4), Sep 1992. in press.

[18] V.S. Anishchenko, M.A. Safonova, and L.O. Chua. Stochastic resonance in Chua's circuit. *Int. J. of Bifurcation and Chaos*, 2(2):397–401, June 1992.

[19] K.S. Halle, L.O. Chua, V.S. Anishchenko, and M.A. Safonova. Signals application via chaos. *Int. J. of Bifurcation and Chaos*, 2(4), Dec 1992. in press.

[20] M.P. Kennedy. Experimental chaos via Chua's circuit. *S. Vohra et al (Editors). Proc. of the 1st Experimental chaos conference, World Scientific*, pages 340–351, 1992.

[21] M.P. Kennedy. Robust op amp realization of Chua's circuit. *Frequenz*, 46(34):66–80, 1992.

[22] J. Cruz and L.O. Chua. A CMOS IC nonlinear resistor for Chua's circuit. *IEEE Trans CAS*, 39(11), 1992. in press.

[23] A.I. Khibnik, D. Roose, and L.O. Chua. On periodic orbits and homoclinic bifurcations in Chua's circuit with smooth nonlinearity. *J. of Circuits, Systems and Computers*, 3(2), June 1992. in press.

[24] R. Brown. From Chua's circuit to the generalized Chua map. *J. of Circuits, Systems and Computers*, 3(1), March 1993. in press.

[25] M. Misiurewicz. Unimodal interval maps obtained from the modified Chua equations. *J. of Circuits, Systems and Computers*, 3(2), June 1993. in press.

[26] V. Perez-Munuzuri, V. Perez-Villar, and L.O. Chua. Autowaves for image processing on a 2-dimensional CNN array of Chua's circuits. *IEEE Trans CAS*, 39(3), March 1993. in press.

[27] F. Zou and J.A. Nossek. An autonomous chaotic neural network and Chua's circuit. *IEEE Trans CAS*, 39(3), March 1993. in press.

[28] Lj. Kocarev, Lj. Karadzinov, and L.O. Chua. N-dimensional canonical Chua's circuit. *J. of Circuits, Systems and Computers*, 3(1), March 1993. in press.

[29] K.A Lukin. High frequency oscillation from Chua's circuit. *J. of Circuits, Systems and Computers*, 3(2), June 1992. in press.

[30] A.N. Sharkovsky, Yu. Maistrenko, P. Deregel, and L.O. Chua. Dry turbulence from a time-delayed Chua's circuit. *J. of Circuits, Systems and Computers*, 3(2), June 1992. in press.

[31] L.P. Shil'nikov. Strange attractors and dynamical models. *J. of Circuits, Systems and Computers*, 3(1), March 1992. in press.

[32] V.N. Belykh and L.O. Chua. New type of strange attractor from a geometric model of Chua's circuit. *Int. J. of Bifurcation and Chaos*, 2(3):697–704, Sept 1992.

[33] E.J. Altman. Bifurcation analysis of Chua's circuit with applications for low-level visual sensing. *J. of Circuits, Systems and Computers*, 3(1), March 1993. in press.

[34] X. Rodet. Sound and music from Chua's circuit. *J. of Circuits, Systems and Computers*, 3(1), March 1993. in press.

[35] T. Matsumoto, L.O. Chua, and R Tokunaga. Chaos via torus breakdown. *IEEE Trans CAS*, 34(3):240–253, 1987.

[36] P. Bartissol and L.O. Chua. The double hook. *IEEE Trans CAS*, 35(12):1212–1522, Dec.1988.

[37] M.J. Ogorzalek. Order and chaos in a third-order RC ladder network with nonlinear feedback. *IEEE Trans CAS*, 36(9):1221–1230, 1989.

[38] Y. Nishio, N. Inaba, and S. Mori. Chaotic phenomena in an autonomous circuit with nonlinear inductor. *ISCAS*, 1990.

[39] Y. Nishio, N. Inaba, S. Mori, and T. Saito. Rigorous analysis of windows in a symmetric circuit. *IEEE Trans CAS*, 37(4):473–487, April 1990.

[40] F. Zou and J. A. Nossek. An autonomous chaotic cellular neural network and Chua's circuit. *J. of Circuits, Systems and Computers*, 3(2), June 1993. in press.

[41] A. Avneodo, P. Coullet, and C. Tresser. Possible new strange attractors with spiral structure. *Communications in Mathematical Physics*, 79:573–579, 1981.

[42] R.W. Brockett. On conditions leading to chaos in feedback systems. *Proc. CDC*, pages 932–936, December 1982.

[43] C.T. Sparrow. Chaos in three-dimensional single loop feedback systems with a piecewise-linear feedback function. *J. of Mathematical analysis and applications*, 83(1):275–291, 1981.

[44] D.K. Arrowsmith and C. M. Place. An introduction to dynamical systems. *Cambridge University Press*, Cambridge, UK, 1990.

[45] L.O.Chua and G.N. Lin. Canonical realization of Chua's circuit family. *IEEE Trans CAS*, 37(7):885–902, July 1990.

[46] P. Hartman. *Ordinary Differential Equations.* Birkhauser, Boston, second edition, 1982.

[47] L. O. Chua and R. Ying. Canonical piecewise-linear analysis. *IEEE Trans CAS*, 3(3):125–140, 1983.

[48] T.S. Parker and L.O. Chua. *Practical Numerical Algorithms for Chaotic Systems.* Springer - verlag, New York, 1989.

[49] L.O. Chua. *Introduction to Nonlinear Network Theory.* McGraw Hill, New York, 1969.

[50] L.O. Chua, Desoer C.A., and E.S. Kuh. *Linear and Nonlinear Circuits.* McGraw Hill, New York, 1987.

[51] L. O. Chua and F. Ayrom. Designing nonlinear single op - amp circuits : A cookbook approach. *Int. J. of Circuit Theory and Applications*, 13(3):235 – 268, July 1985.

[52] L. O. Chua and S. Wong. Synthesis of piecewise-linear network. *Journal on Electronic Circuits and Systems*, 2(4):102–108, 1978.

Figure Captions

Fig.1. (a) Chua's circuit.

(b) v-i characteristic of the nonlinear resistor(drawn with $G_a < G_b \leq 0$)

Fig.2. (a) unfolded canonical circuit. The nonlinear resistor may be characterized by any piecewise continuous function. For the family $\mathcal{C}$ of vector fields studied in this paper, this is assumed to be piecewise-linear, such as shown in Fig.1(b), where

$G_a < G_b \leq 0$, or

(b) $G_b < G_a < 0$,

(c) $G_a < 0, \ G_b > 0$,

(d) $G_b > G_a > 0$,

(e) $G_a > 0, \ G_b < 0$, and

(f) $G_a > G_b > 0$.

Fig.3. (a) Strange attractor reproduced from Fig.3 of Ref.[38].

(b) Equivalent strange attractor generated by the unfolded Chua's Circuit with parameters given by Eq.(48).

Fig.4. (a) Strange attractor reproduced from Fig.9 (page 936) of Ref.[42].

(b) Qualitatively similar Equivalent strange attractor generated by the unfolded Chua's Circuit with parameters given by Eq.(50).

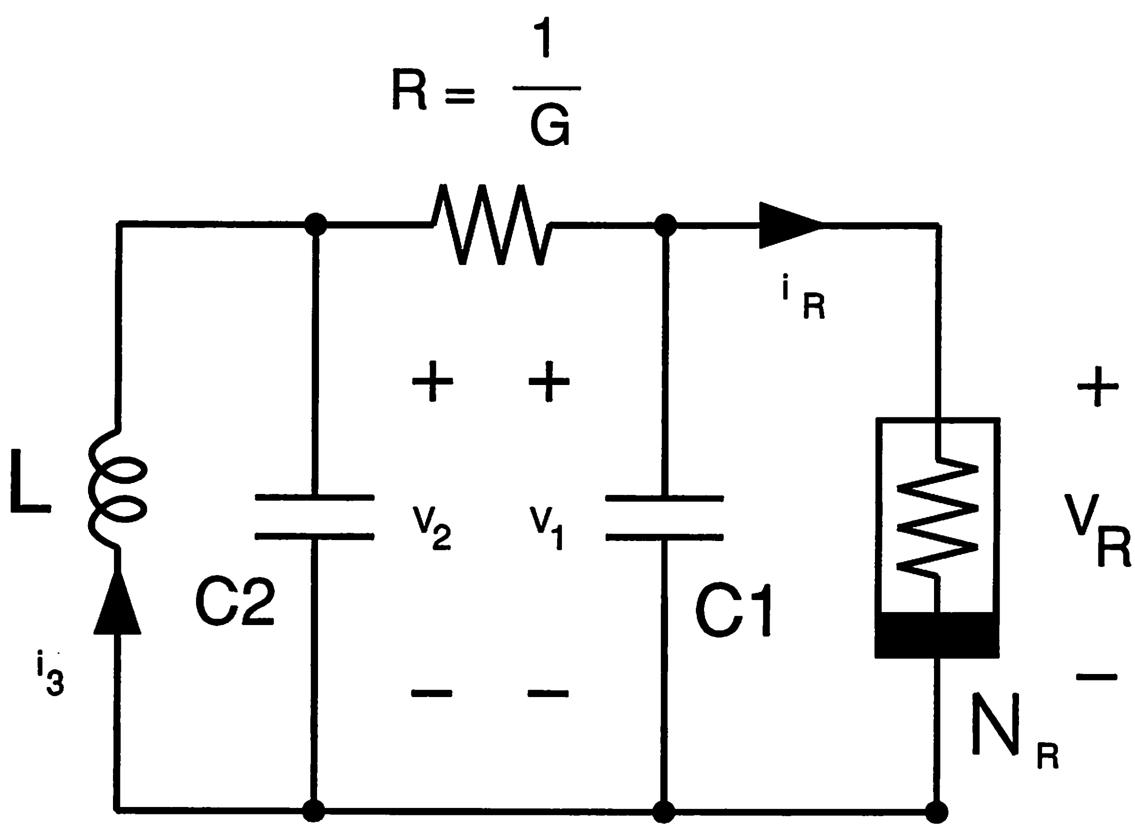

Figure 1a

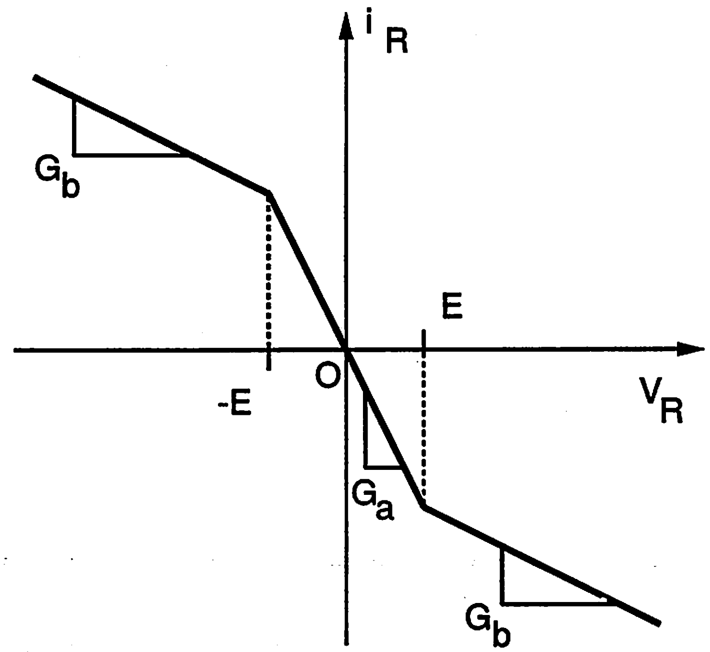

Figure 1b

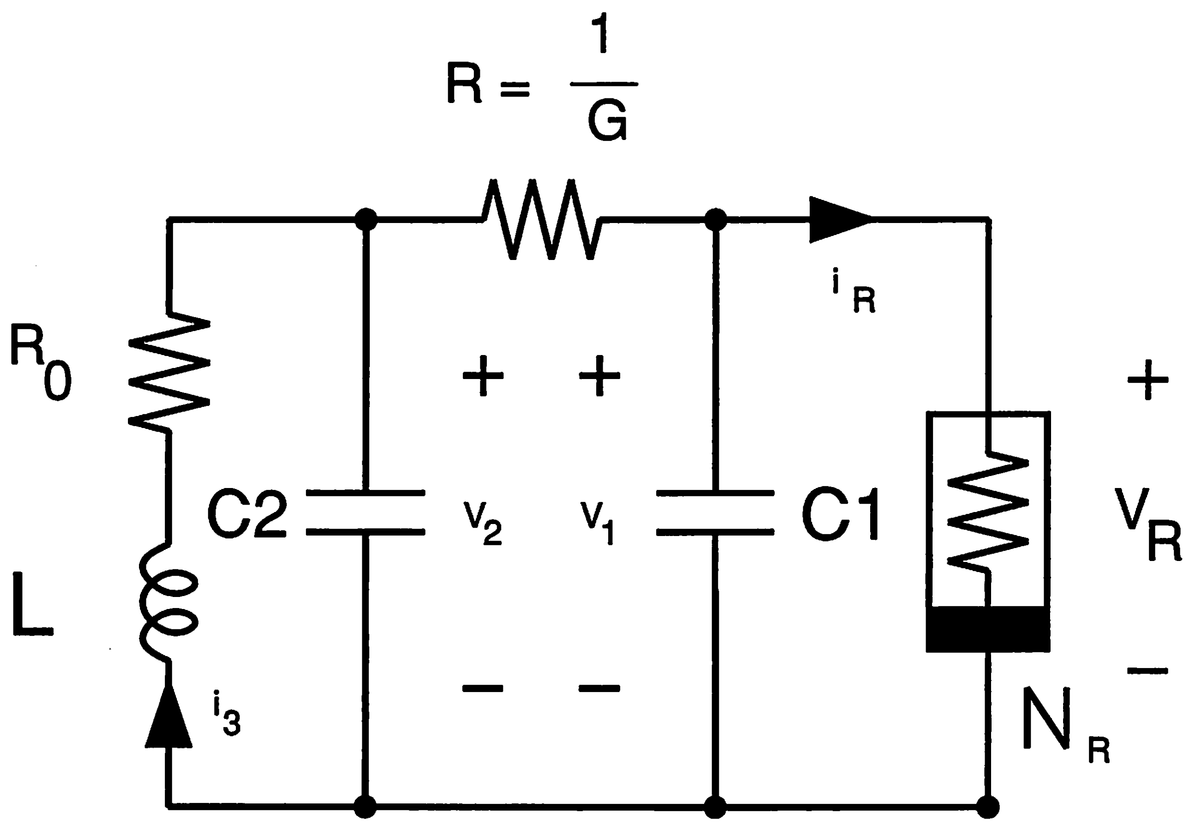

Figure 2a

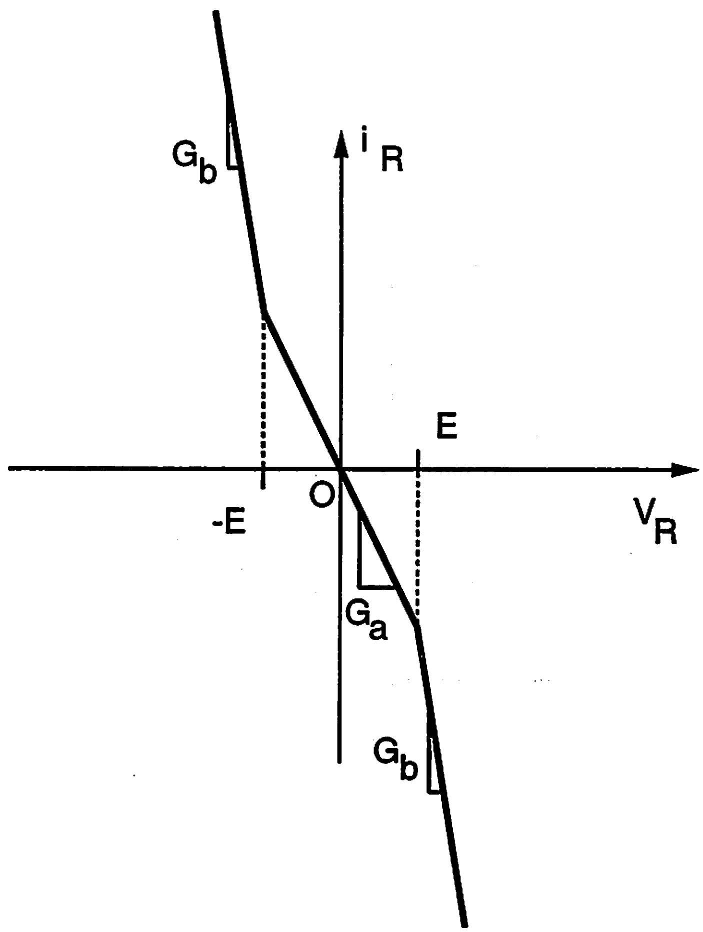

Figure 2b

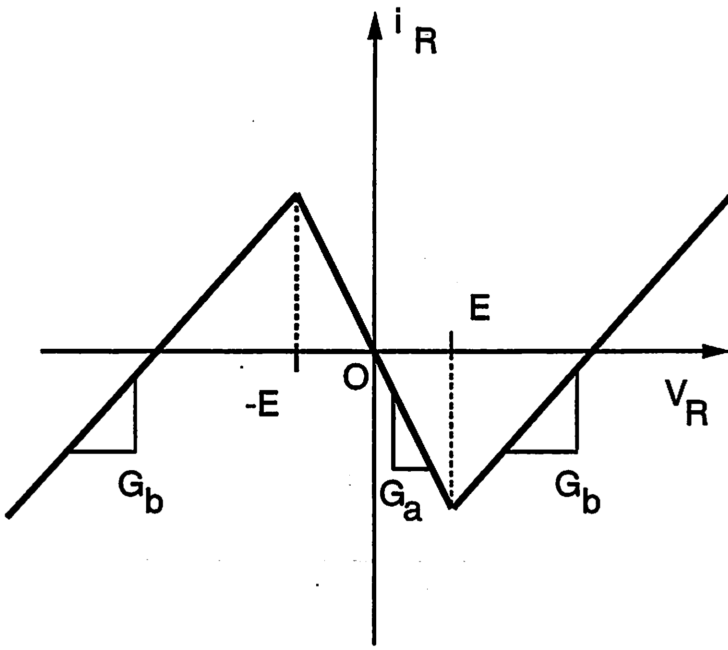

Figure 2c

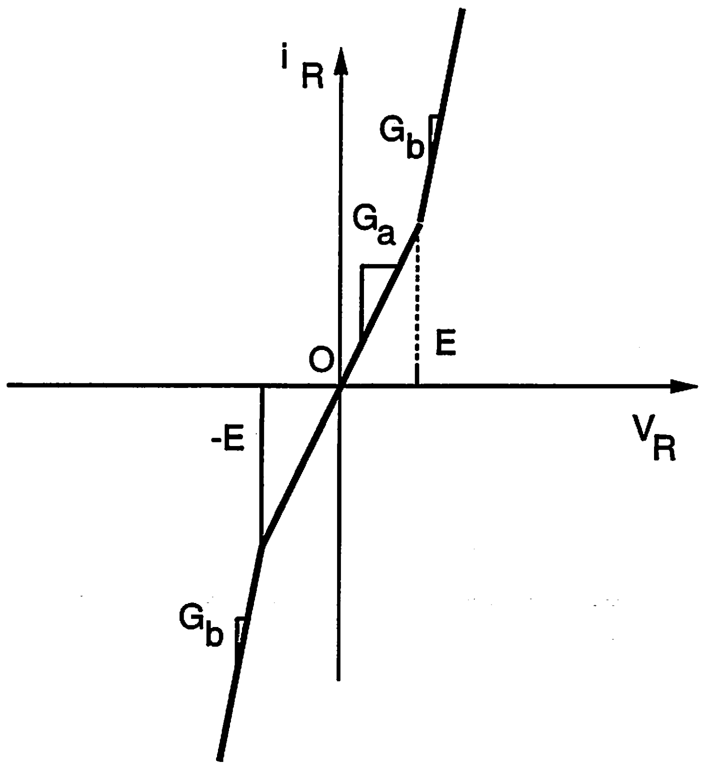

Figure 2d

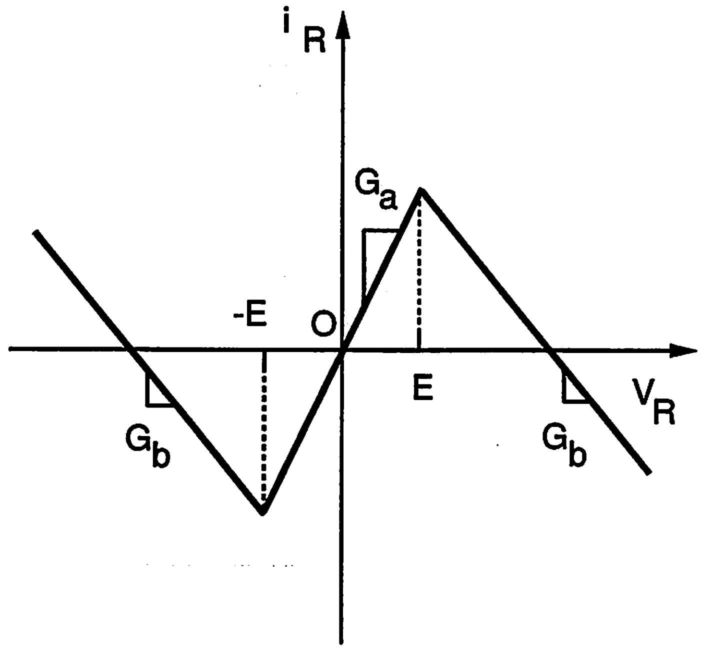

Figure 2e

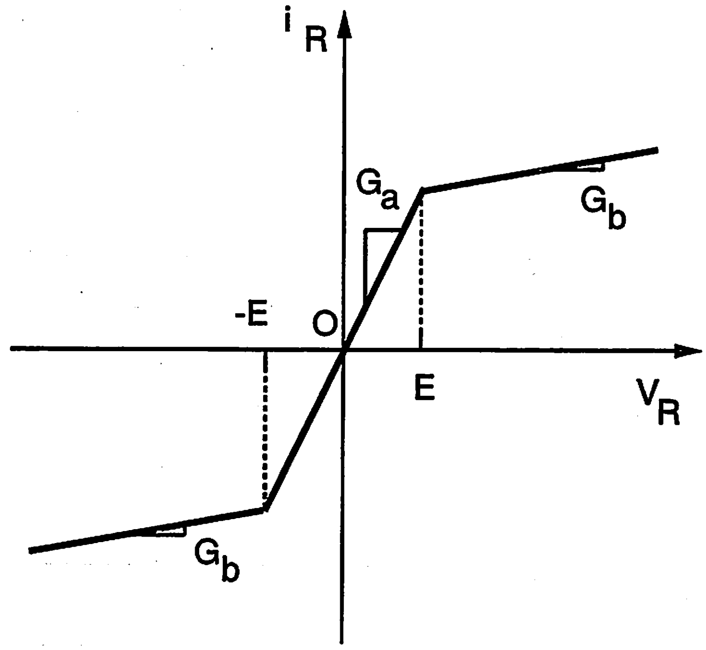

Figure 2f

Fig. 3 (a) Strange attractor reproduced from Fig. 3 of Ref. [38]. (b) Equivalent strange attractor generated by the unfolded Chua's circuit with parameters given by Eq. (48).

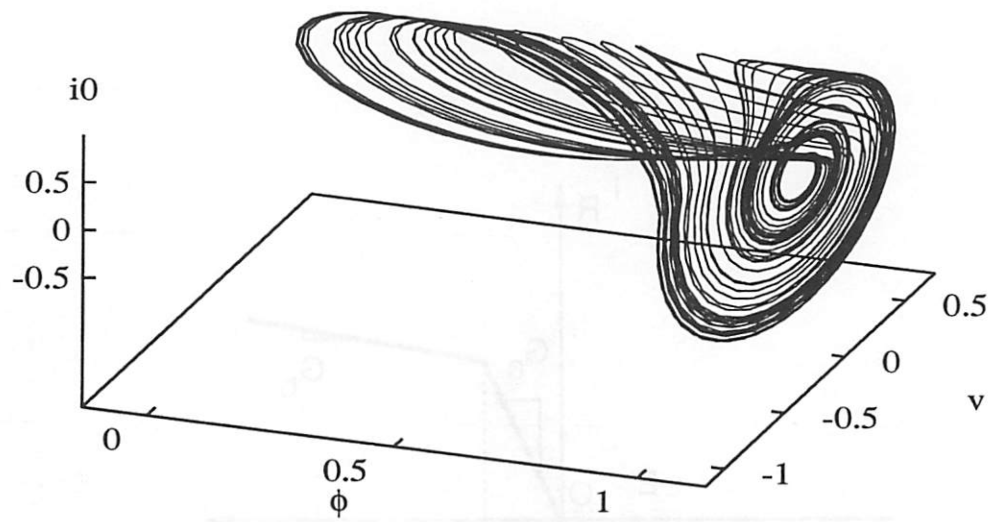

(a)

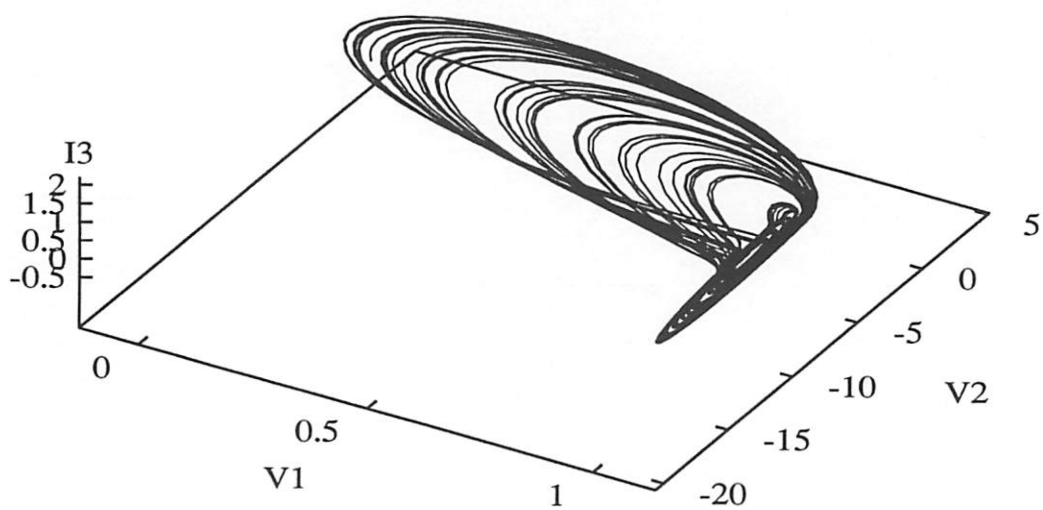

(b)

Fig. 4 (a) Strange attractor reproduced from Fig. 9 (page 936) of Ref. [42]. (b) Qualitatively similar strange attractor generated by the unfolded Chua's circuit with parameters given by Eq. (50).

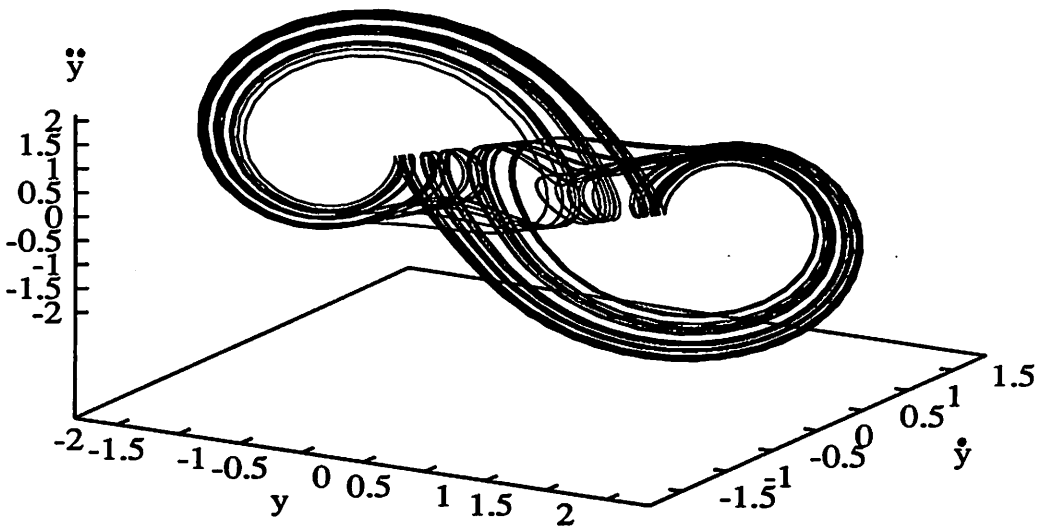

(a)

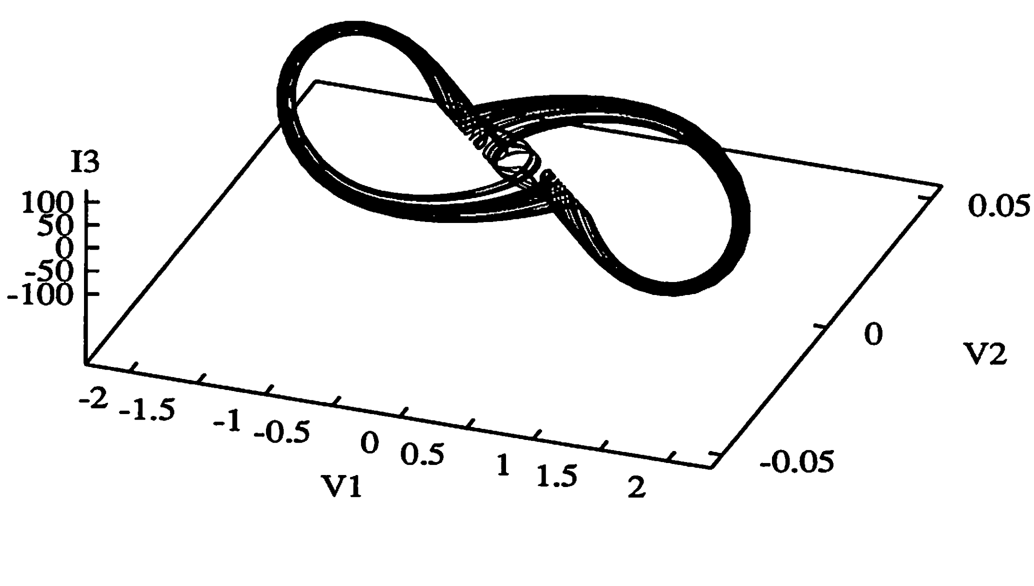

(b)

Table 1 Attractors from Chua's circuit. In the 3-D phase portraits, the units on the V_1 and V_2 axes are volts, and the units on the I_3 axis is milliamps. $E = 1v$.

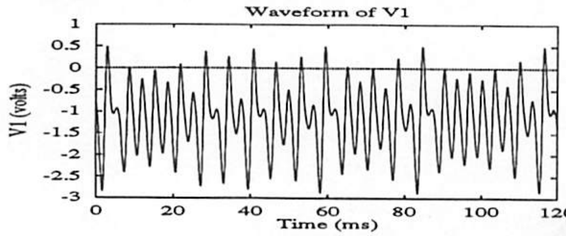

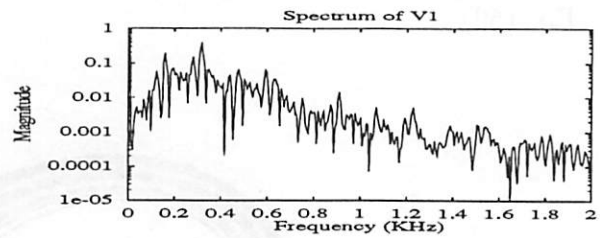

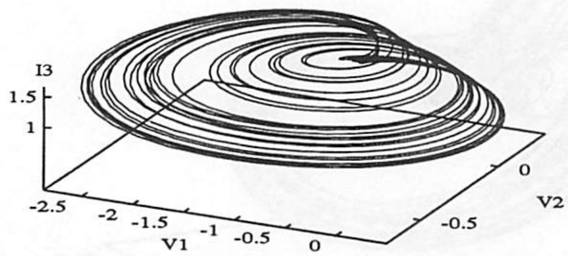

1.1 $C_1 = -149nF$, $C_2 = 1\mu F$, $L = -658mH$, $G_a = -1.14mS$, $G_b = -0.714mS$, $R = 1K\Omega$. **Eigenvalues:** $\mu_1 = 16.4$, $\mu_2 = -1.08 \times 10^3 + 2.33 \times 10^3 j$, $\mu_3 = -1.08 \times 10^3 - 2.33 \times 10^3 j$, $\nu_1 = -672$, $\nu_2 = 796 + 1.93 \times 10^3 j$, $\nu_3 = 796 - 1.93 \times 10^3 j$.

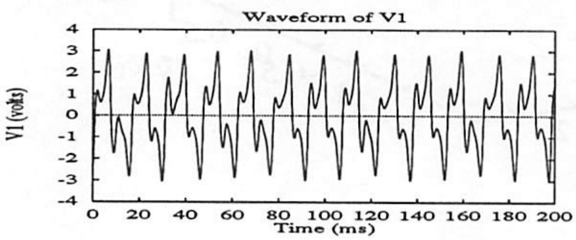

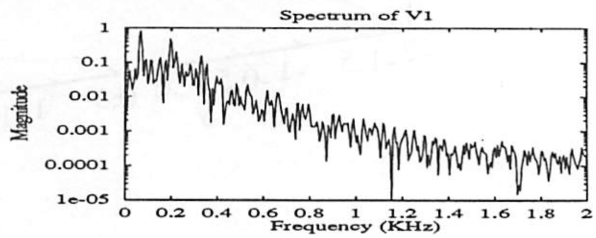

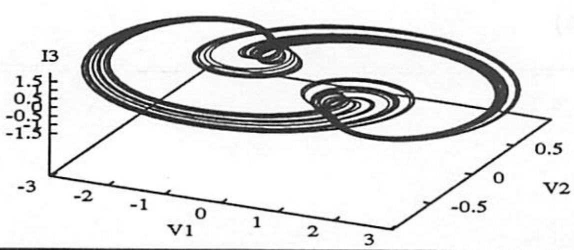

1.2 $C_1 = -245nF$, $C_2 = 1\mu F$, $L = -500mH$, $G_a = -1.14292mS$, $G_b = -0.7142mS$, $R = 1K\Omega$. **Eigenvalues:** $\mu_1 = 599$, $\mu_2 = -1.67 \times 10^3 + 1.74 \times 10^3 j$, $\mu_3 = -1.67 \times 10^3 - 1.74 \times 10^3 j$, $\nu_1 = -1.06 \times 10^3$, $\nu_2 = 612 + 1.35 \times 10^3 j$, $\nu_3 = 612 - 1.35 \times 10^3 j$.

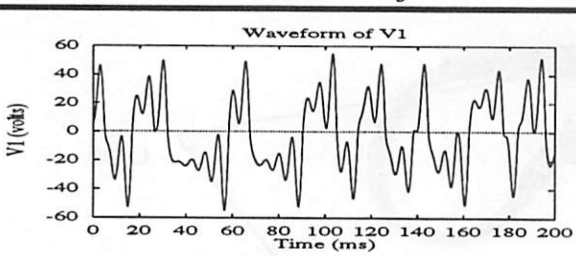

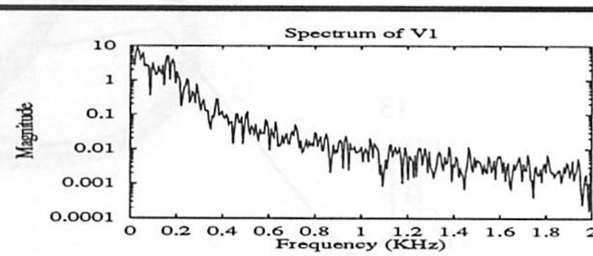

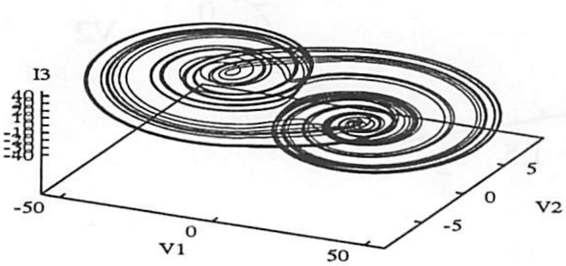

1.3 $C_1 = -203nF$, $C_2 = 1\mu F$, $L = -274mH$, $G_a = -2.497mS$, $G_b = -0.9301mS$, $R = 1K\Omega$. **Eigenvalues:** $\mu_1 = -6.34 \times 10^3$, $\mu_2 = -3.31 \times 10^3$, $\mu_3 = 1.28 \times 10^3$, $\nu_1 = -992$, $\nu_2 = 168 + 1.11 \times 10^3 j$, $\nu_3 = 168 - 1.11 \times 10^3 j$.

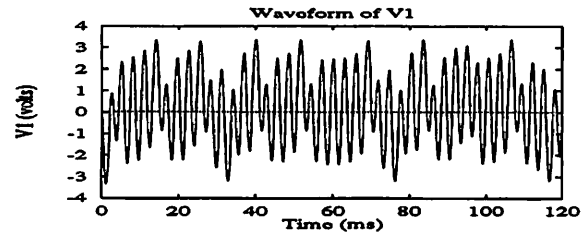

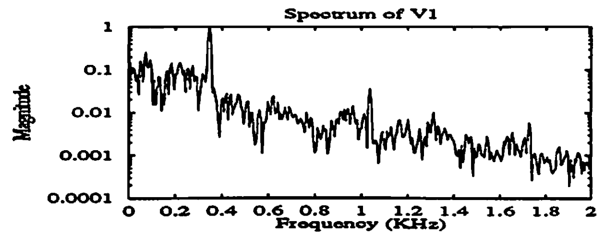

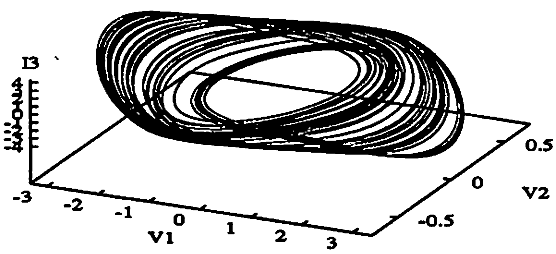

1.4 $C_1 = 120nF$, $C_2 = 1\mu F$, $L = 83.9mH$, $G_a = -0.7048mS$, $G_b = -1.146mS$, $R = 1K\Omega$.
Eigenvalues: $\mu_1 = -3.86 \times 10^3$, $\mu_2 = 200 + 2.75 \times 10^3 j$, $\mu_3 = 200 - 2.75 \times 10^3 j$, $\nu_1 = 2.18 \times 10^3$, $\nu_2 = -982 + 2.39 \times 10^3 j$, $\nu_3 = -982 - 2.39 \times 10^3 j$.

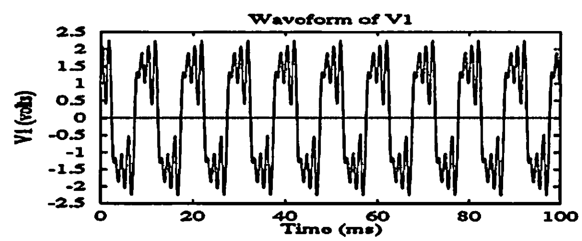

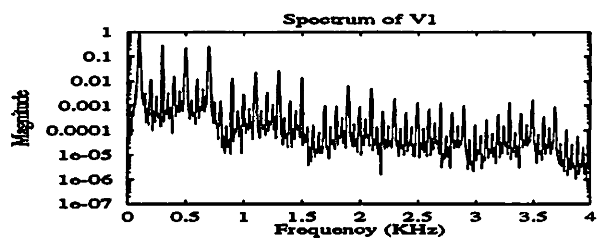

1.5 $C_1 = 64.1nF$, $C_2 = 1\mu F$, $L = 35mH$, $G_a = -1.143mS$, $G_b = -0.7143mS$, $R = 1K\Omega$. Initial Conditions: $v_1 = 1.8035v$, $v_2 = 0.1804v$, $i_3 = -1.8797mA$.
Eigenvalues: $\mu_1 = 7.95 \times 10^3$, $\mu_2 = -1.12 \times 10^3 + 4.48 \times 10^3 j$, $\mu_3 = -1.12 \times 10^3 - 4.48 \times 10^3 j$, $\nu_1 = -6.05 \times 10^3$, $\nu_2 = 298 + 4.58 \times 10^3 j$, $\nu_3 = 298 - 4.58 \times 10^3 j$.

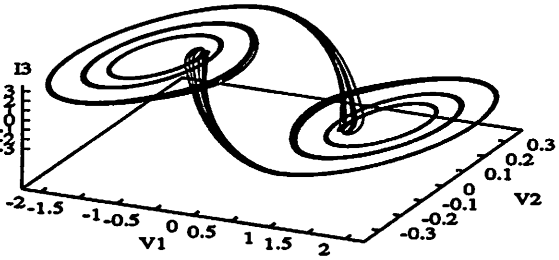

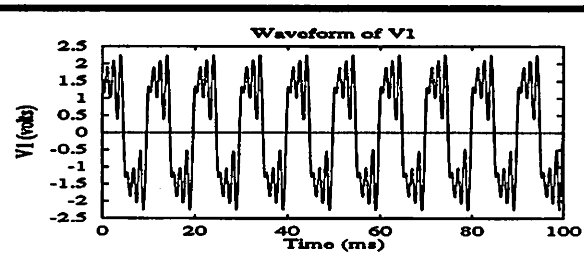

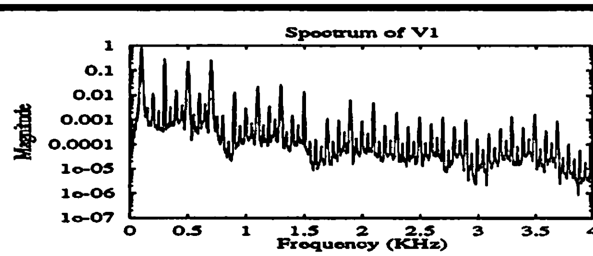

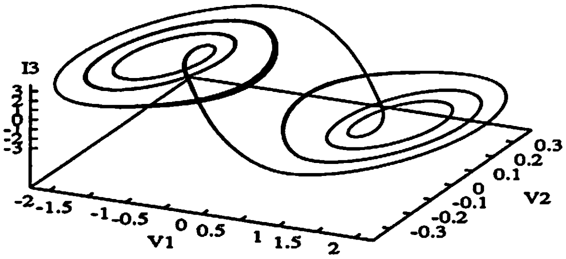

1.6 $C_1 = 64.1nF$, $C_2 = 1\mu F$, $L = 35mH$, $G_a = -1.143mS$, $G_b = -0.7143mS$, $R = 1K\Omega$. Initial Conditions: $v_1 = 1.1638v$, $v_2 = -0.09723$, $i_3 = -0.90565mA$.
Eigenvalues: $\mu_1 = 7.95 \times 10^3$, $\mu_2 = -1.12 \times 10^3 + 4.48 \times 10^3 j$, $\mu_3 = -1.12 \times 10^3 - 4.48 \times 10^3 j$, $\nu_1 = -6.05 \times 10^3$, $\nu_2 = 298 + 4.58 \times 10^3 j$, $\nu_3 = 298 - 4.58 \times 10^3 j$.

Table 2 Period doubling route to Chaos. The fixed parameters are $R_0 = 0\Omega$, $R = 1K\Omega$, $L = 6.25mH$, $Ga = -1.143mS$, $Gb = -0.714mS$, $C2 = 100nF$, $E = 1v$. In the 3-D phase portraits, the units on the V_1 and V_2 axes are volts, and the units on the I_3 axis is milliamps.

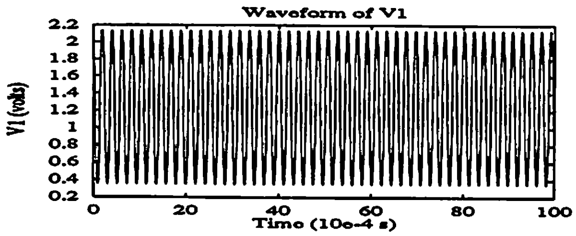

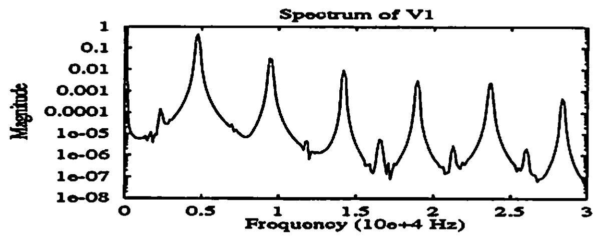

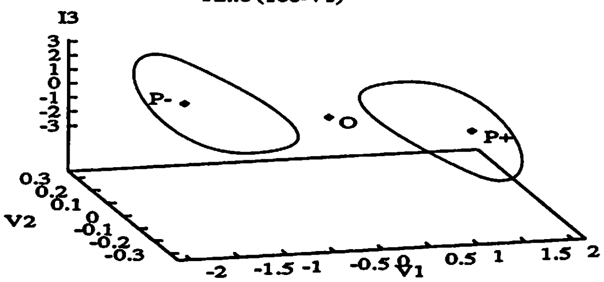

2.1 Control parameter: $C1 = 11.364nF$. **Eigenvalues:** $\mu_1 = 2.07 \times 10^4$, $\mu_2 = -9.68 \times 10^3 + 2.98 \times 10^4 j$, $\mu_3 = -9.68 \times 10^3 - 2.98 \times 10^4 j$, $\nu_1 = -3.77 \times 10^4$, $\nu_2 = 1.27 \times 10^3 + 3.27 \times 10^4 j$, $\nu_3 = 1.27 \times 10^3 - 3.27 \times 10^4 j$.

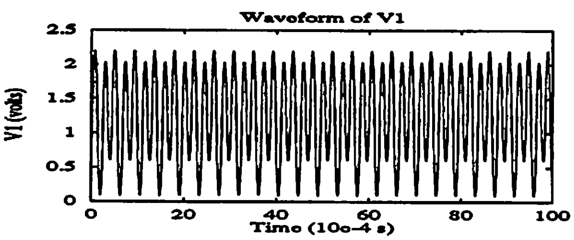

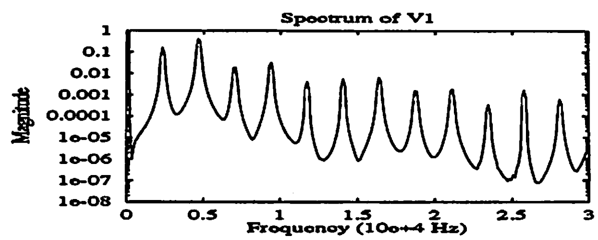

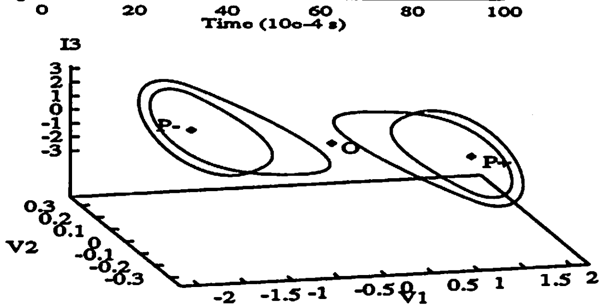

2.2 Control parameter: $C1 = 11.050nF$. **Eigenvalues:** $\mu_1 = 2.15 \times 10^4$, $\mu_2 = -9.27 \times 10^3 + 2.97 \times 10^4 j$, $\mu_3 = -9.27 \times 10^3 - 2.97 \times 10^4 j$, $\nu_1 = -3.88 \times 10^4$, $\nu_2 = 1.40 \times 10^3 + 3.26 \times 10^4 j$, $\nu_3 = 1.40 \times 10^3 - 3.26 \times 10^4 j$.

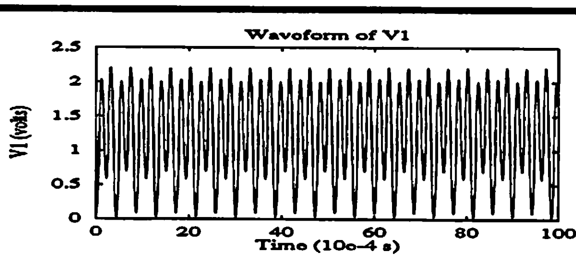

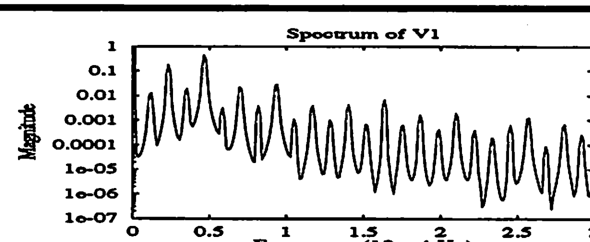

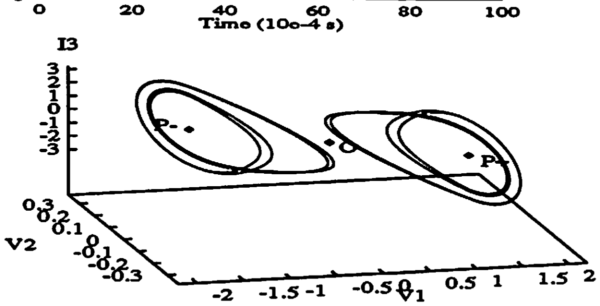

2.3 Control parameter: $C1 = 10.965nF$. **Eigenvalues:** $\mu_1 = 2.17 \times 10^4$, $\mu_2 = -9.32 \times 10^3 + 2.96 \times 10^4 j$, $\mu_3 = -9.32 \times 10^3 - 2.96 \times 10^4 j$, $\nu_1 = -3.91 \times 10^4$, $\nu_2 = 1.51 \times 10^3 + 3.26 \times 10^4 j$, $\nu_3 = 1.51 \times 10^3 - 3.26 \times 10^4 j$.

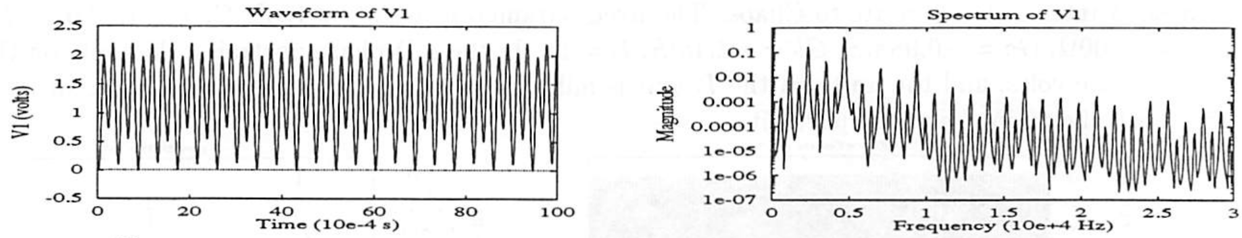

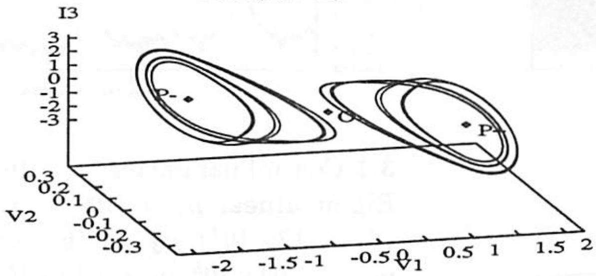

2.4 Control parameter: $C1 = 10.915nF$. **Eigenvalues:** $\mu_1 = 2.18 \times 10^4$, $\mu_2 = -9.36 \times 10^3 + 2.96 \times 10^4 j$, $\mu_3 = -9.36 \times 10^3 - 2.96 \times 10^4 j$, $\nu_1 = -3.93 \times 10^4$, $\nu_2 = 1.54 \times 10^3 + 3.26 \times 10^4 j$, $\nu_3 = 1.54 \times 10^3 - 3.26 \times 10^4 j$.

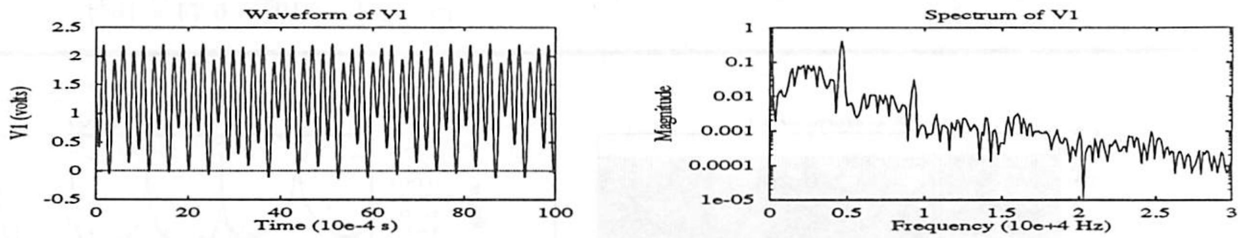

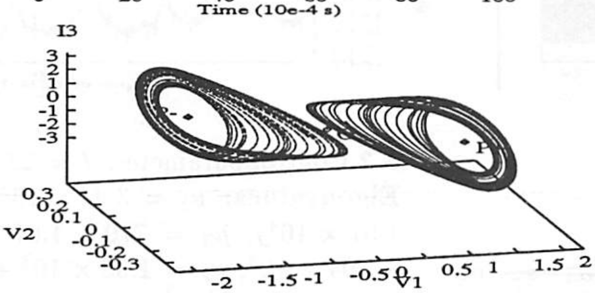

2.5 Control parameter: $C1 = 10.753nF$. **Eigenvalues:** $\mu_1 = 2.22 \times 10^4$, $\mu_2 = -9.46 \times 10^3 + 2.95 \times 10^4 j$, $\mu_3 = -9.46 \times 10^3 - 2.95 \times 10^4 j$, $\nu_1 = -3.99 \times 10^4$, $\nu_2 = 1.64 \times 10^3 + 3.26 \times 10^4 j$, $\nu_3 = 1.64 \times 10^3 - 3.26 \times 10^4 j$.

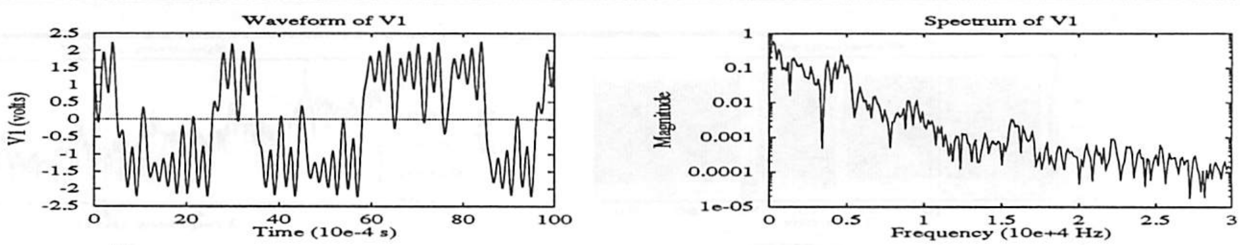

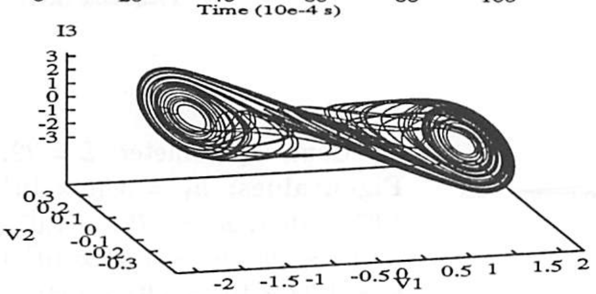

2.6 Control parameter: $C1 = 10.204nF$. **Eigenvalues:** $\mu_1 = 2.37 \times 10^4$, $\mu_2 = -9.84 \times 10^3 + 2.91 \times 10^4 j$, $\mu_3 = -9.84 \times 10^3 - 2.91 \times 10^4 j$, $\nu_1 = -4.20 \times 10^4$, $\nu_2 = 1.99 \times 10^3 + 3.26 \times 10^4 j$, $\nu_3 = 1.99 \times 10^3 - 3.26 \times 10^4 j$.

Table 3 Intermittency route to Chaos. The fixed parameters are $C_2 = 1\mu F$, $C_1 = -13.33nF$, $R = 1K\Omega$, $R_0 = -100\Omega$, $Ga = -0.98mS$, $Gb = -2.4mS$, $E = 1v$. In the 3-D phase portraits, the units on the V_1 and V_2 axes are volts, and the units on the I_3 axis is milliamps. In 3.2, the asymmetric attractor and its twin are both shown in the phase portrait.

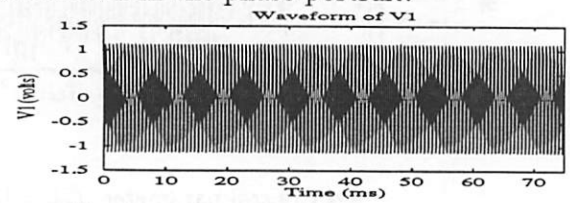

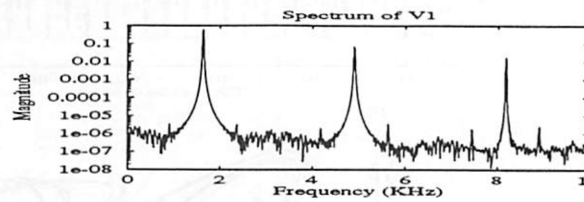

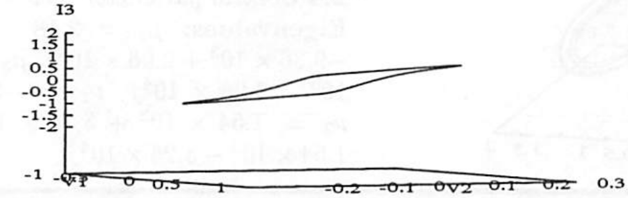

3.1 Control parameter: $L = 16.67mH$.
Eigenvalues: $\mu_1 = 4.19 \times 10^3$, $\mu_2 = 1.16 \times 10^3 + 1.12 \times 10^4 j$, $\mu_3 = 1.16 \times 10^3 - 1.12 \times 10^4 j$, $\nu_1 = -1.04 \times 10^5$, $\nu_2 = 2.14 \times 10^3 + 6.74 \times 10^3 j$, $\nu_3 = 2.14 \times 10^3 - 6.74 \times 10^3 j$.

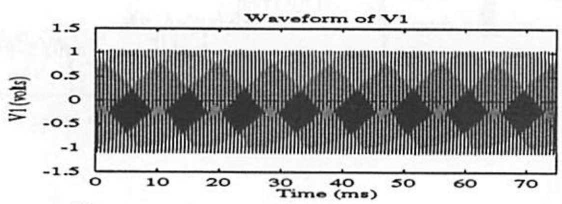

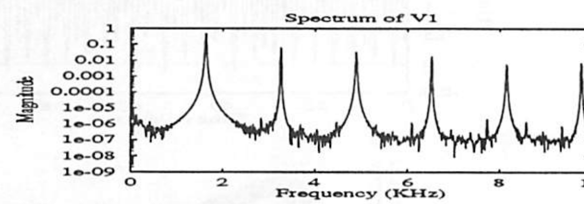

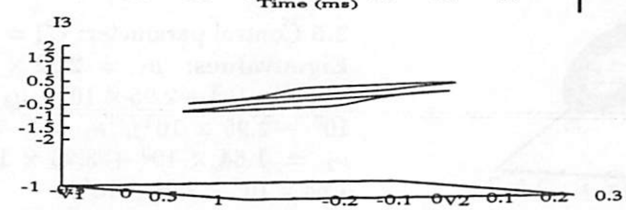

3.2 Control parameter: $L = 22.32mH$.
Eigenvalues: $\mu_1 = 3.44 \times 10^3$, $\mu_2 = 770 + 1.07 \times 10^4 j$, $\mu_3 = 770 - 1.07 \times 10^4 j$, $\nu_1 = -1.04 \times 10^5$, $\nu_2 = 1.38 \times 10^3 + 5.96 \times 10^3 j$, $\nu_3 = 1.38 \times 10^3 - 5.96 \times 10^3 j$.

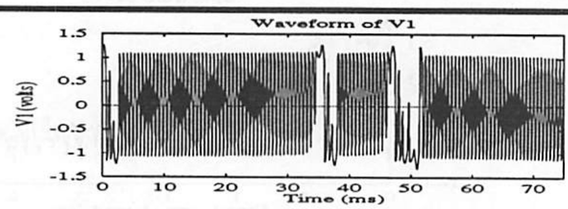

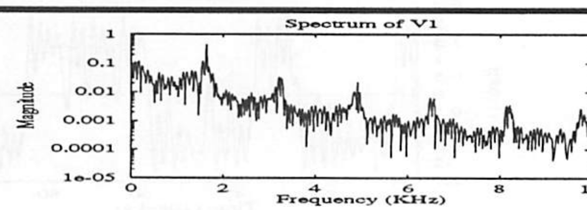

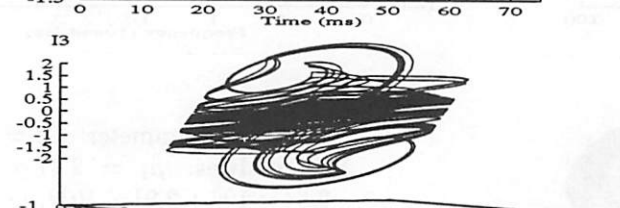

3.3 Control parameter: $L = 22.73mH$.
Eigenvalues: $\mu_1 = 3.40 \times 10^3$, $\mu_2 = 751 + 1.07 \times 10^4 j$, $\mu_3 = 751 - 1.07 \times 10^4 j$, $\nu_1 = -1.04 \times 10^5$, $\nu_2 = 1.34 \times 10^3 + 5.91 \times 10^3 j$, $\nu_3 = 1.34 \times 10^3 - 5.91 \times 10^3 j$.

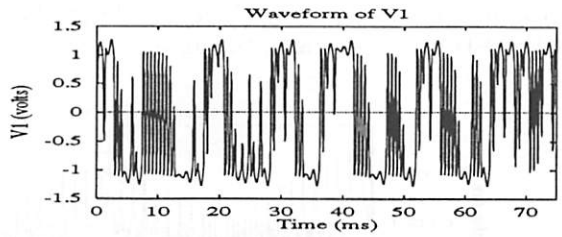

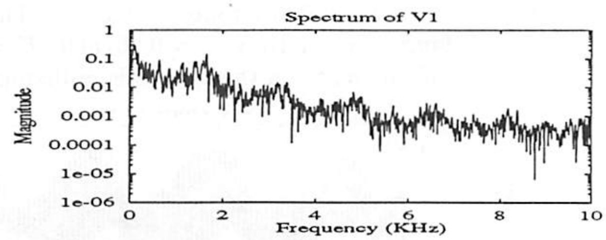

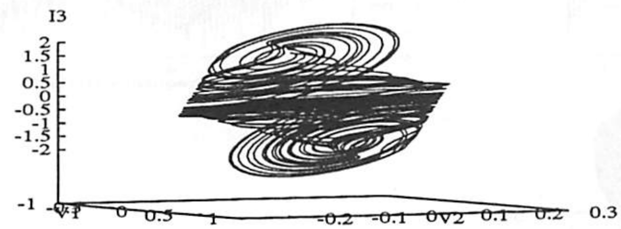

3.4 Control parameter: $L = 28.80mH$. **Eigenvalues:** $\mu_1 = 2.88 \times 10^3$, $\mu_2 = 548 + 1.03 \times 10^4 j$, $\mu_3 = 548 - 1.03 \times 10^4 j$, $\nu_1 = -1.04 \times 10^5$, $\nu_2 = 874 + 5.31 \times 10^3 j$, $\nu_3 = 874 - 5.31 \times 10^3 j$.

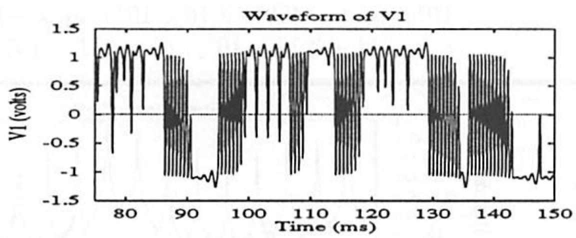

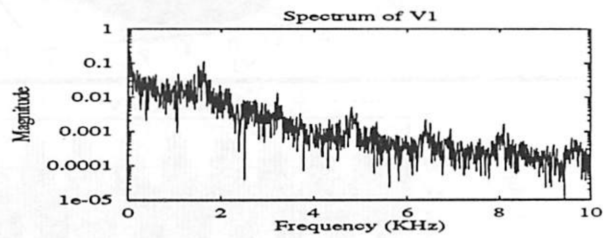

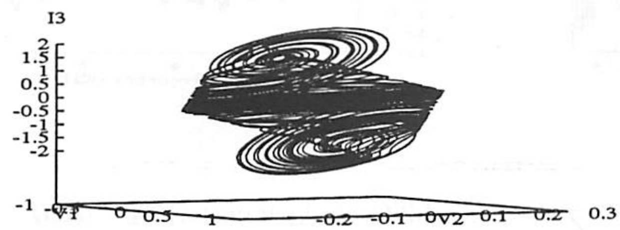

3.5 Control parameter: $L = 31.50mH$. **Eigenvalues:** $\mu_1 = 2.70 \times 10^3$, $\mu_2 = 489 + 1.02 \times 10^4 j$, $\mu_3 = 489 - 1.02 \times 10^4 j$, $\nu_1 = -1.04 \times 10^5$, $\nu_2 = 725 + 5.10 \times 10^3 j$, $\nu_3 = 725 - 5.10 \times 10^3 j$.

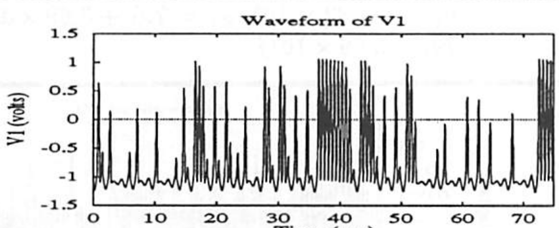

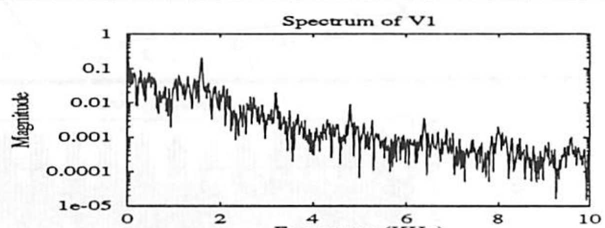

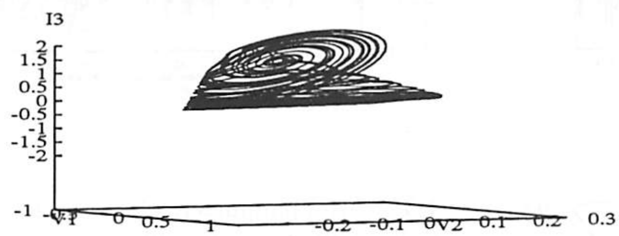

3.6 Control parameter: $L = 32.00mH$. **Eigenvalues:** $\mu_1 = 2.67 \times 10^3$, $\mu_2 = 480 + 1.02 \times 10^4 j$, $\mu_3 = 480 - 1.02 \times 10^4 j$, $\nu_1 = -1.04 \times 10^5$, $\nu_2 = 700 + 5.06 \times 10^3 j$, $\nu_3 = 700 - 5.06 \times 10^3 j$.

Table 4 Torus breakdown route to Chaos. The fixed parameters are $C_2 = 1\mu F$, $R = -1K\Omega$, $R_0 = 0.651\Omega$, $Ga = 0.856mS$, $Gb = 1.1mS$, $L = 0.667mH$, $E = 1v$. In the 3-D phase portraits, the units on the V_1 and V_2 axes are volts, and the units on the I_3 axis is milliamps.

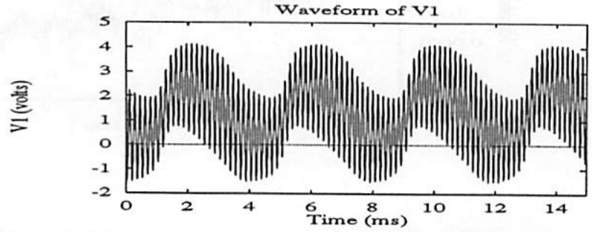

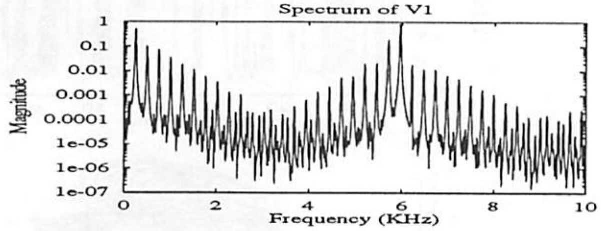

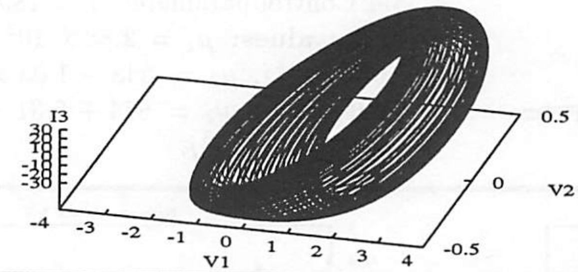

4.1 Control parameter: $C_1 = 10nF$.
Eigenvalues: $\mu_1 = 1.53\times10^4$, $\mu_2 = -459+3.76\times10^4j$, $\mu_3 = -459-3.76\times10^4j$, $\nu_1 = -1.06\times10^4$, $\nu_2 = 311+3.75\times10^4j$, $\nu_3 = 311-3.75\times10^4j$.

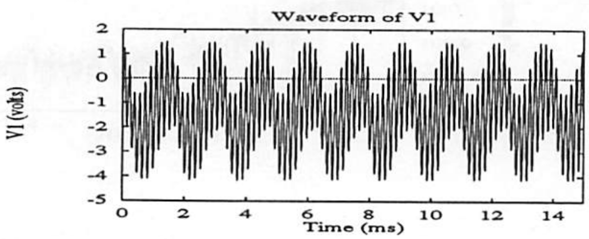

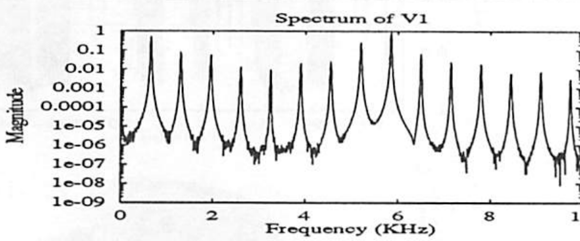

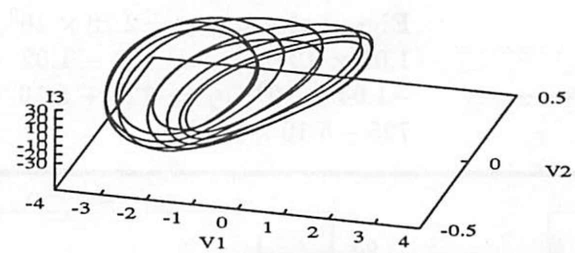

4.2 Control parameter: $C_1 = 6.0nF$.
Eigenvalues: $\mu_1 = 2.61\times10^4$, $\mu_2 = -1.03\times10^3+3.72\times10^4j$, $\mu_3 = -1.03\times10^3-3.72\times10^4j$, $\nu_1 = -1.82\times10^4$, $\nu_2 = 797+3.69\times10^4j$, $\nu_3 = 797-3.69\times10^4j$.

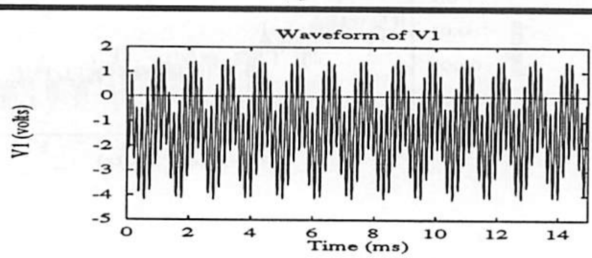

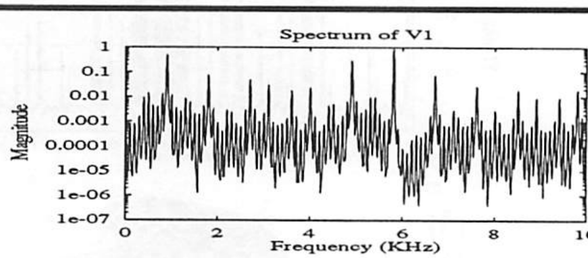

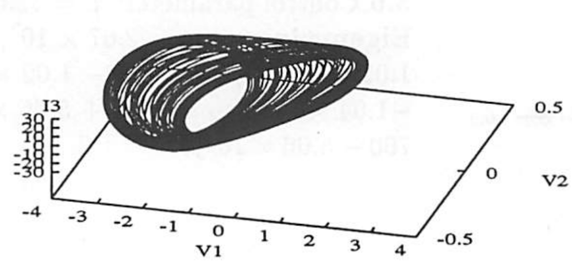

4.3 Control parameter: $C_1 = 5.1nF$.
Eigenvalues: $\mu_1 = 3.08\times10^4$, $\mu_2 = -1.26\times10^3+3.71\times10^4j$, $\mu_3 = -1.26\times10^3-3.71\times10^4j$, $\nu_1 = -2.17\times10^4$, $\nu_2 = 1.04\times10^3+3.67\times10^4j$, $\nu_3 = 1.04\times10^3-3.67\times10^4j$.

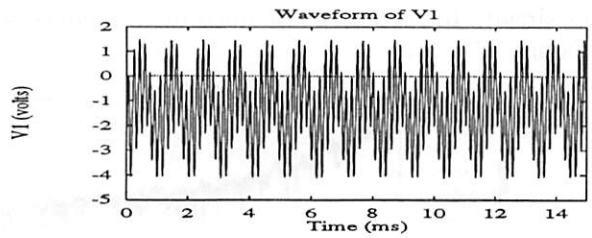

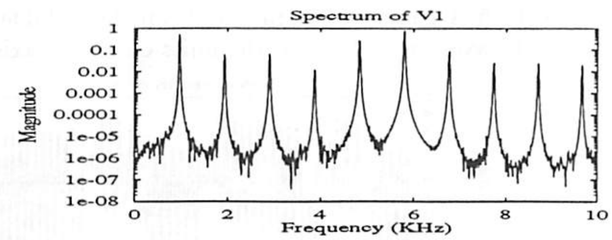

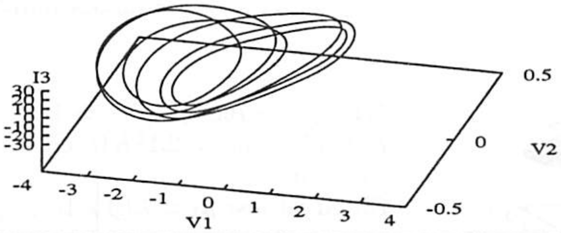

4.4 Control parameter: $C_1 = 5.0nF$.
Eigenvalues: $\mu_1 = 3.14 \times 10^4$, $\mu_2 = -1.29 \times 10^3 + 3.71 \times 10^4 j$, $\mu_3 = -1.29 \times 10^3 - 3.71 \times 10^4 j$, $\nu_1 = -2.21 \times 10^4$, $\nu_2 = 1.08 \times 10^3 + 3.67 \times 10^4 j$, $\nu_3 = 1.08 \times 10^3 - 3.67 \times 10^4 j$.

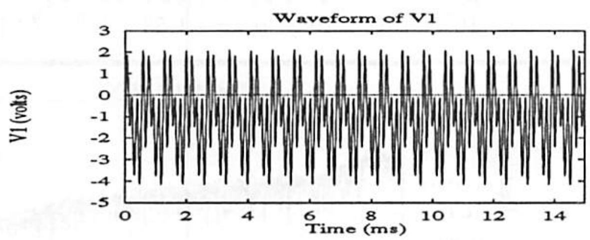

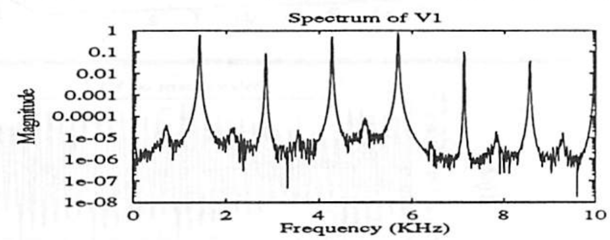

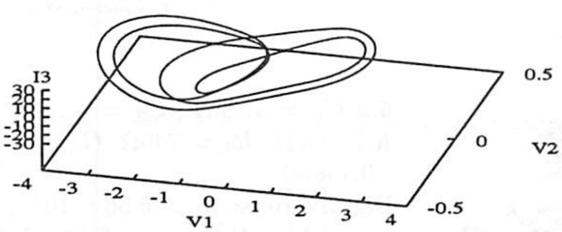

4.5 Control parameter: $C_1 = 3.5nF$.
Eigenvalues: $\mu_1 = 4.49 \times 10^4$, $\mu_2 = -1.85 \times 10^3 + 3.71 \times 10^4 j$, $\mu_3 = -1.85 \times 10^3 - 3.71 \times 10^4 j$, $\nu_1 = -3.21 \times 10^4$, $\nu_2 = 1.77 \times 10^3 + 3.64 \times 10^4 j$, $\nu_3 = 1.77 \times 10^3 - 3.64 \times 10^4 j$.

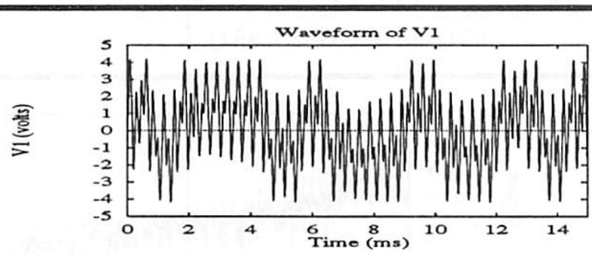

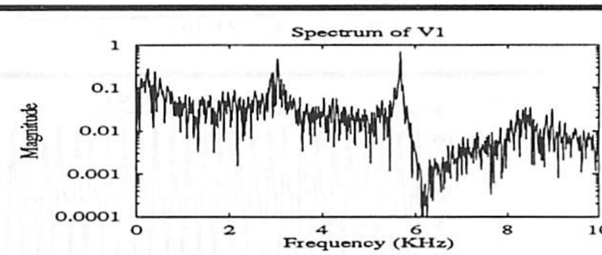

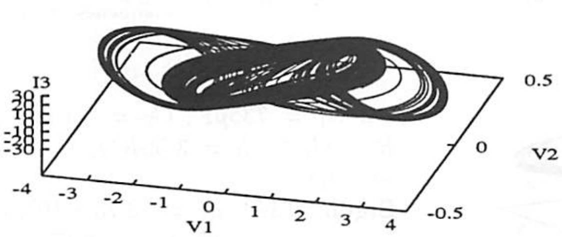

4.6 Control parameter: $C_1 = 2.94nF$.
Eigenvalues: $\mu_1 = 5.33 \times 10^4$, $\mu_2 = -2.12 \times 10^3 + 3.72 \times 10^4 j$, $\mu_3 = -2.12 \times 10^3 - 3.72 \times 10^4 j$, $\nu_1 = -3.83 \times 10^4$, $\nu_2 = 2.15 \times 10^3 + 3.63 \times 10^4 i$, $\nu_3 = 2.15 \times 10^3 - 3.63 \times 10^4 j$.

Table 5 A gallery of attractors from the unfolded Chua's circuit. In the 3-D phase portraits, the units on the V_1 and V_2 axes are volts, and the units on the I_3 axis is milliamps. $E = 1v$.

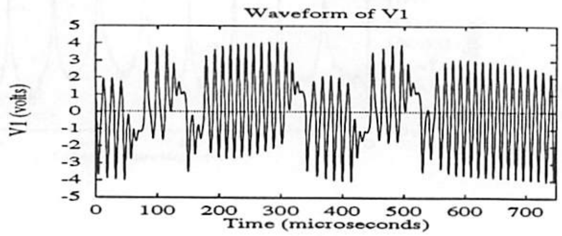

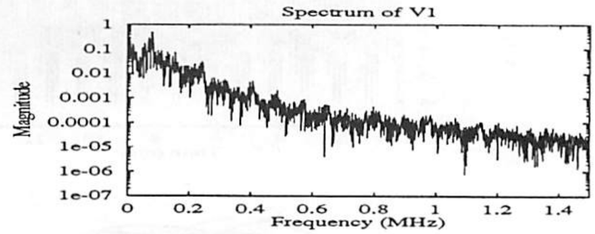

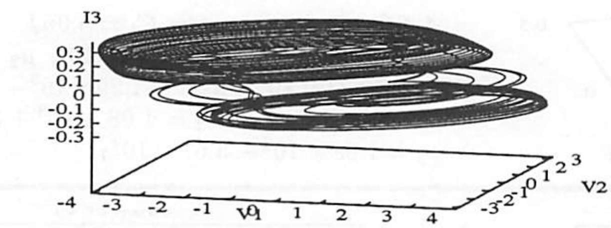

5.1 $C_1 = -768.6pF$, $C_2 = 1nF$, $L = -73.5mH$, $R = 1K\Omega$, $R_0 = 2.18K\Omega$, $G_a = 0.169mS$, $G_b = -0.477mS$.
Eigenvalues: $\mu_1 = 7.84 \times 10^5$, $\mu_2 = -3.37 \times 10^5$, $\mu_3 = 1.03 \times 10^5$, $\nu_1 = 1.52 \times 10^4$, $\nu_2 = -1.53 \times 10^5 + 7.61 \times 10^5 j$, $\nu_3 = -1.53 \times 10^5 - 7.61 \times 10^5 j$.

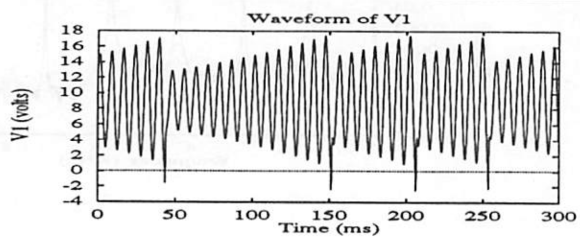

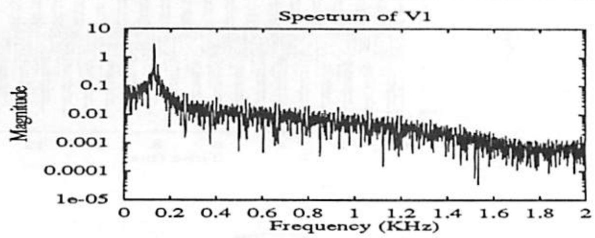

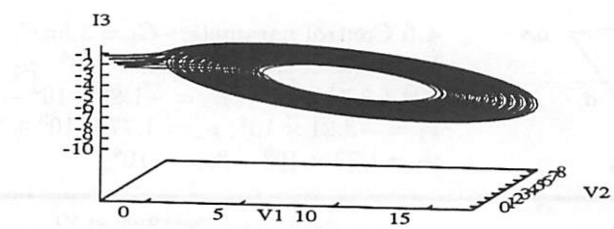

5.2 $C_1 = 57.5nF$, $C_2 = -1\mu F$, $L = -708mH$, $R = 1K\Omega$, $R_0 = 740\Omega$, $G_a = -1.525mS$, $G_b = -0.458mS$.
Eigenvalues: $\mu_1 = 5.56 \times 10^3$, $\mu_2 = 3.61 \times 10^3$, $\mu_3 = 1.57 \times 10^3$, $\nu_1 = -7.40 \times 10^3$, $\nu_2 = -18.2 + 854j$, $\nu_3 = -18.2 - 854j$.

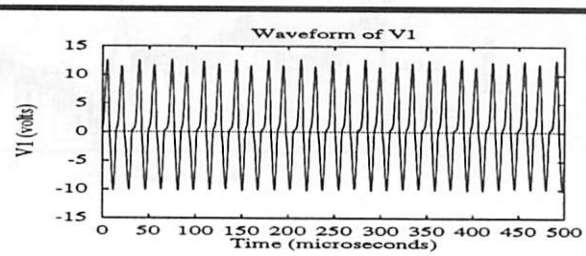

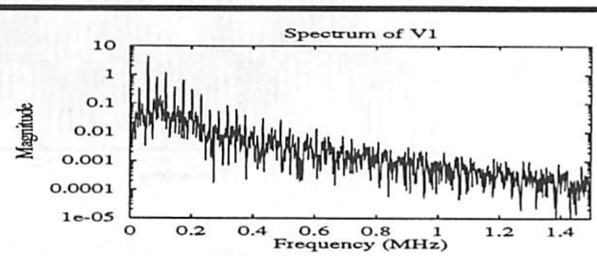

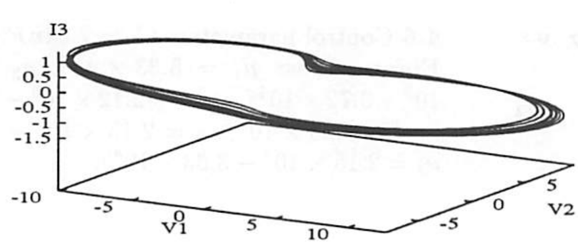

5.3 $C_1 = 735pF$, $C_2 = -1nF$, $L = 11.44mH$, $R = 1K\Omega$, $R_0 = 3.56K\Omega$, $G_a = 1.292mS$, $G_b = -0.497mS$.
Eigenvalues: $\mu_1 = -2.75 \times 10^6$, $\mu_2 = 7.30 \times 10^5$, $\mu_3 = -4.08 \times 10^5$, $\nu_1 = -2.67 \times 10^5$, $\nu_2 = 1.36 \times 10^5 + 7.38 \times 10^5 j$, $\nu_3 = 1.36 \times 10^5 - 7.38 \times 10^5 j$.

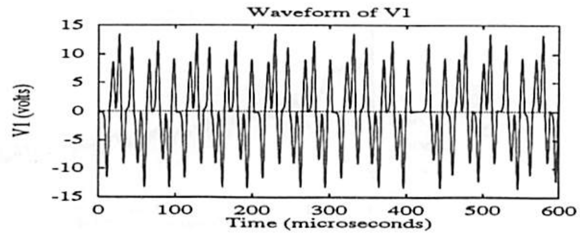

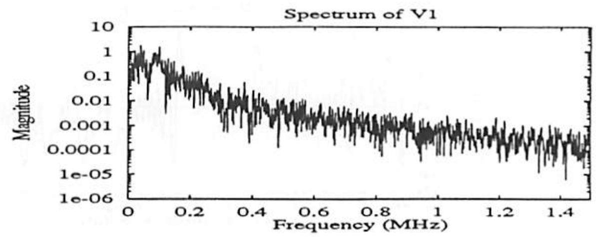

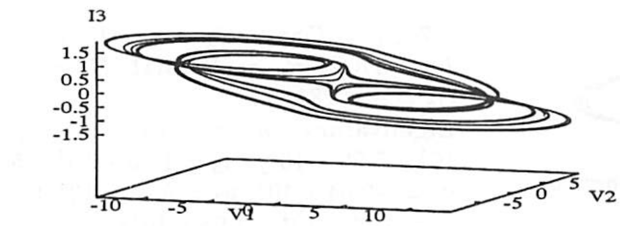

5.4 $C_1 = 684pF$, $C_2 = -1nF$, $L = 10.6mH$, $R = 1K\Omega$, $R_0 = 3.43K\Omega$, $G_a = 1.219mS$, $G_b = -0.514mS$.

Eigenvalues: $\mu_1 = -2.86 \times 10^6$, $\mu_2 = 7.22 \times 10^5$, $\mu_3 = -4.27 \times 10^5$, $\nu_1 = -2.79 \times 10^5$, $\nu_2 = 1.22 \times 10^5 + 7.85 \times 10^5 j$, $\nu_3 = 1.22 \times 10^5 - 7.85 \times 10^5 j$.

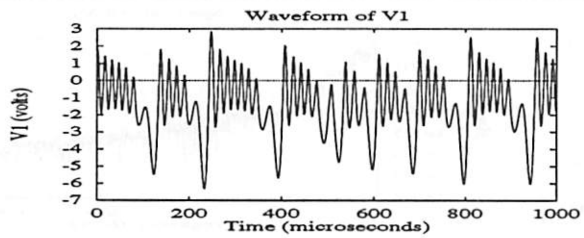

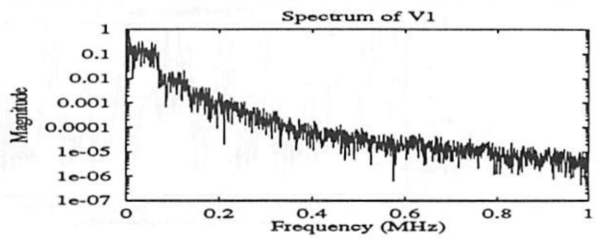

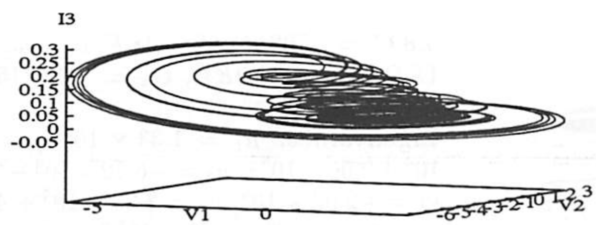

5.5 $C_1 = 811pF$, $C_2 = -1nF$, $L = -138mH$, $R = 1K\Omega$, $R_0 = 12.1K\Omega$, $G_a = -0.177mS$, $G_b = -0.02mS$.

Eigenvalues: $\mu_1 = 5.28 \times 10^4$, $\mu_2 = 1.00 \times 10^4 + 4.72 \times 10^5 j$, $\mu_3 = 1.00 \times 10^4 - 4.72 \times 10^5 j$, $\nu_1 = -2.08 \times 10^5$, $\nu_2 = 4.35 \times 10^4 + 1.73 \times 10^5 j$, $\nu_3 = 4.35 \times 10^4 - 1.73 \times 10^5 j$.

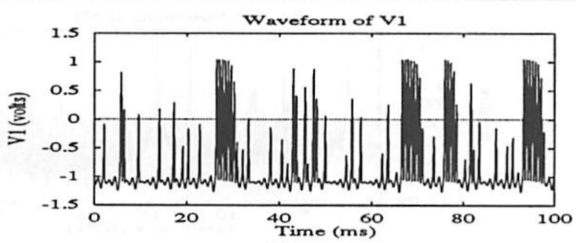

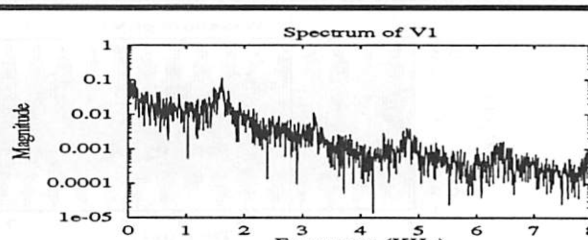

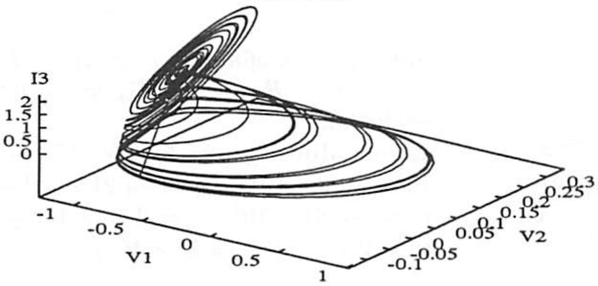

5.6 $C_1 = -13.33nF$, $C_2 = 1\mu F$, $L = 32mH$, $R = 1K\Omega$, $R_0 = -100\Omega$, $G_a = -0.98mS$, $G_b = -2.4mS$.

Eigenvalues: $\mu_1 = 2.67 \times 10^3$, $\mu_2 = 480 + 1.02 \times 10^4 j$, $\mu_3 = 480 - 1.02 \times 10^4 j$, $\nu_1 = -1.04 \times 10^5$, $\nu_2 = 700 + 5.06 \times 10^3 j$, $\nu_3 = 700 - 5.06 \times 10^3 j$.

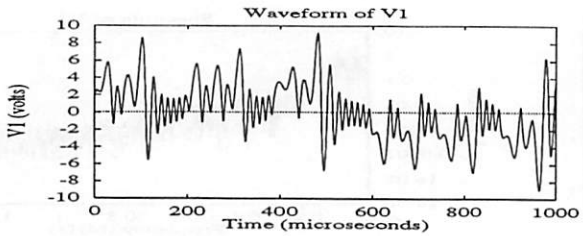

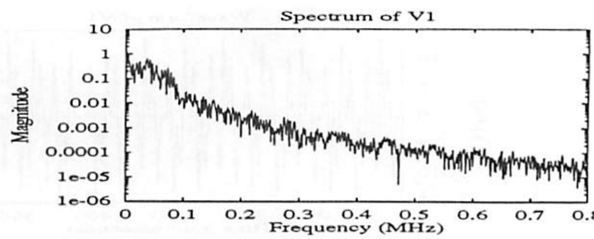

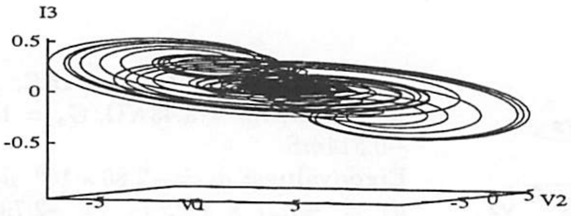

5.7 $C_1 = 758pF$, $C_2 = -1nF$, $L = -79.6mH$, $R = 1K\Omega$, $R_0 = 10.6K\Omega$, $G_a = -0.2241mS$, $G_b = -0.02811mS$.
Eigenvalues: $\mu_1 = 8.75 \times 10^4$, $\mu_2 = 1.10 \times 10^4 + 5.50 \times 10^5 j$, $\mu_3 = 1.10 \times 10^4 - 5.50 \times 10^5 j$, $\nu_1 = -2.64 \times 10^5$, $\nu_2 = 5.74 \times 10^4 + 1.98 \times 10^5 j$, $\nu_3 = 5.74 \times 10^4 - 1.98 \times 10^5 j$.

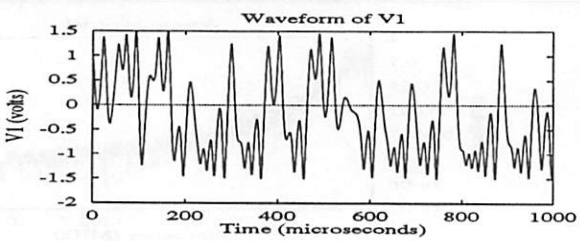

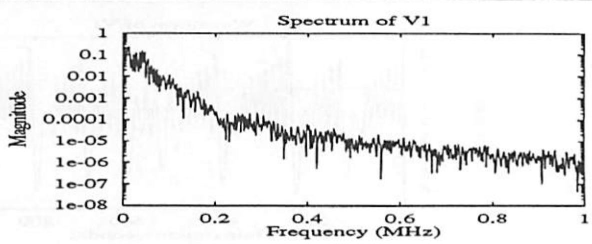

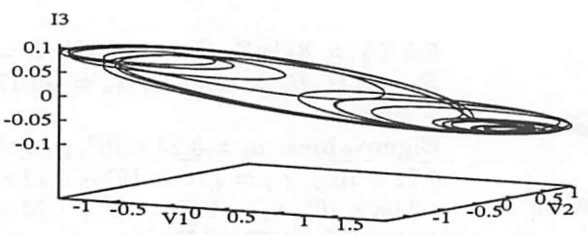

5.8 $C_1 = -702pF$, $C_2 = 1nF$, $L = 33.96mH$, $R = 1K\Omega$, $R_0 = 11.0K\Omega$, $G_a = -0.0715mS$, $G_b = -0.1817mS$.
Eigenvalues: $\mu_1 = 1.33 \times 10^5$, $\mu_2 = -6.72 \times 10^4 + 2.00 \times 10^5 j$, $\mu_3 = -6.72 \times 10^4 - 2.00 \times 10^5 j$, $\nu_1 = -2.03 \times 10^5$, $\nu_2 = 2.25 \times 10^4 + 4.93 \times 10^5 j$, $\nu_3 = 2.25 \times 10^4 - 4.93 \times 10^5 j$.

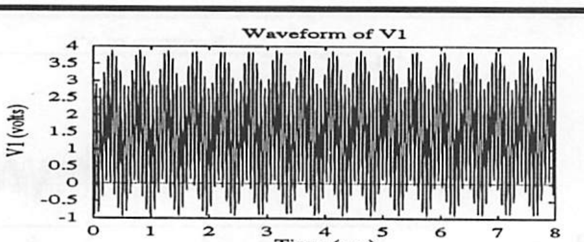

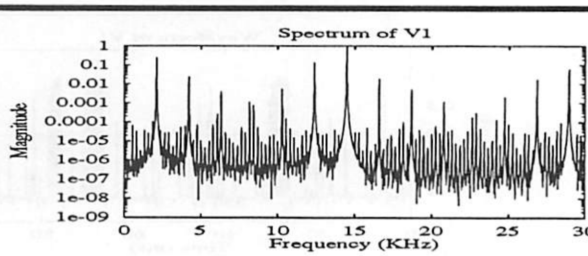

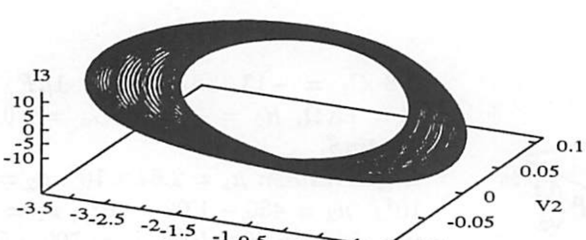

5.9 $C_1 = 0.56nF$, $C_2 = 1\mu F$, $L = 0.1mH$, $R = 1K\Omega$, $R_0 = 0\Omega$, $G_a = -1.026mS$, $G_b = -0.982mS$.
Eigenvalues: $\mu_1 = 5.39 \times 10^4$, $\mu_2 = -4.21 \times 10^3 + 9.28 \times 10^4 j$, $\mu_3 = -4.21 \times 10^3 - 9.28 \times 10^4 j$, $\nu_1 = -3.81 \times 10^4$, $\nu_2 = 2.48 \times 10^3 + 9.18 \times 10^4 j$, $\nu_3 = 2.48 \times 10^3 - 9.18 \times 10^4 j$.

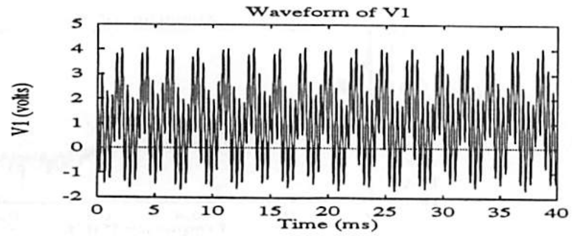

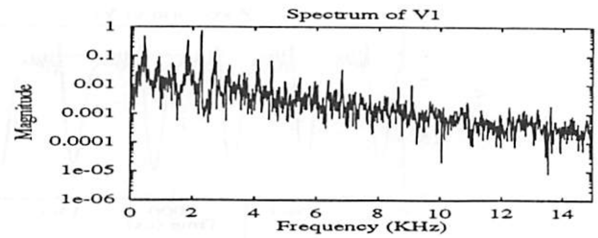

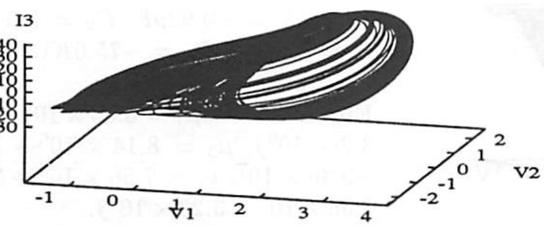

5.10 $C_1 = 75.1nF$, $C_2 = 1\mu F$, $L = 4.7mH$, $R = -1K\Omega$, $R_0 = 4.41\Omega$, $G_a = -0.474mS$, $G_b = 2.039mS$.
Eigenvalues: $\mu_1 = 2.01 \times 10^4$, $\mu_2 = -197 + 1.44 \times 10^4 j$, $\mu_3 = -197 - 1.44 \times 10^4 j$, $\nu_1 = -1.43 \times 10^4$, $\nu_2 = 244 + 1.43 \times 10^4 j$, $\nu_3 = 244 - 1.43 \times 10^4 j$.

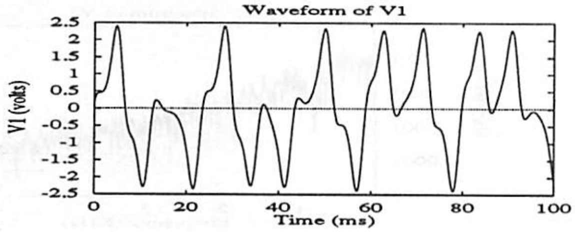

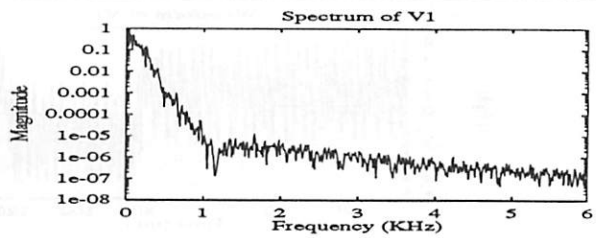

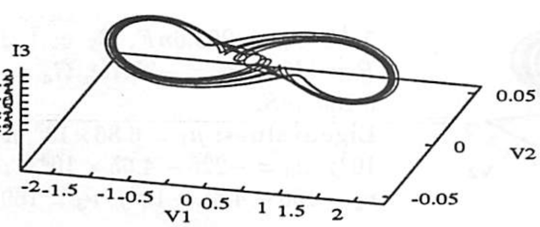

5.11 $C_1 = 19.21nF$, $C_2 = 1\mu F$, $L = 18.42mH$, $R = -1K\Omega$, $R_0 = 18.4\Omega$, $G_a = 1.018mS$, $G_b = 1.02mS$.
Eigenvalues: $\mu_1 = 794$, $\mu_2 = -865 + 1.36 \times 10^4 j$, $\mu_3 = -865 - 1.36 \times 10^4 j$, $\nu_1 = -1.61 \times 10^3$, $\nu_2 = 287 + 1.40 \times 10^3 j$, $\nu_3 = 287 - 1.40 \times 10^3 j$.

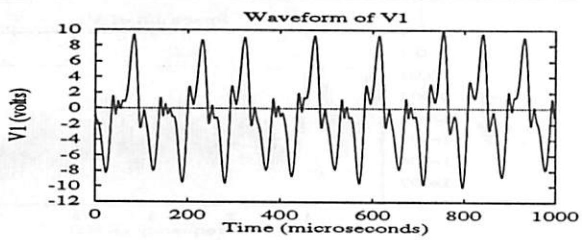

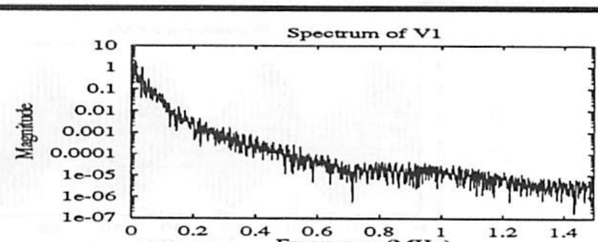

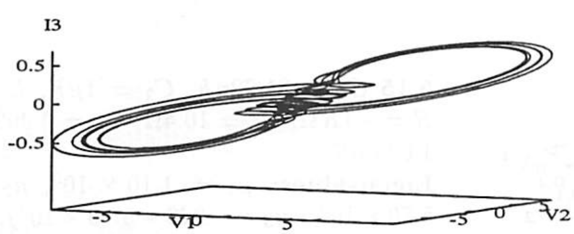

5.12 $C_1 = -641pF$, $C_2 = 1nF$, $L = 63.9mH$, $R = -1K\Omega$, $R_0 = -10.1K\Omega$, $G_a = 0.2438mS$, $G_b = 0.0425mS$.
Eigenvalues: $\mu_1 = 1.09 \times 10^5$, $\mu_2 = -6.54 \times 10^4 + 6.14 \times 10^5 j$, $\mu_3 = -6.54 \times 10^4 - 6.14 \times 10^5 j$, $\nu_1 = -4.05 \times 10^5$, $\nu_2 = 3.45 \times 10^4 + 1.75 \times 10^5 j$, $\nu_3 = 3.45 \times 10^4 - 1.75 \times 10^5 j$.

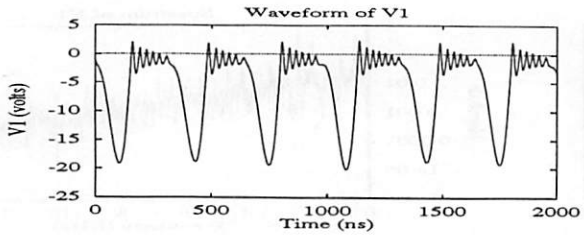

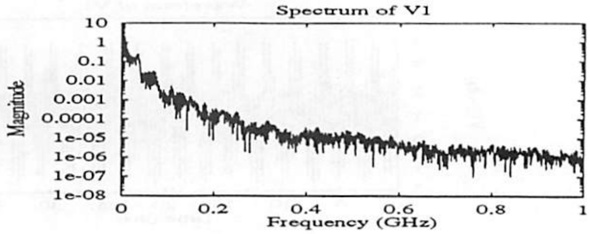

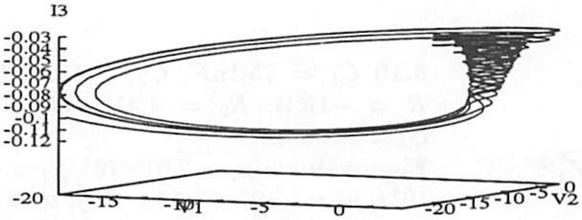

5.13 $C_1 = -0.92pF$, $C_2 = 1pF$, $L = 10.32mH$, $R = -1K\Omega$, $R_0 = -75.6K\Omega$, $G_a = 0.09411mS$, $G_b = 0.1899\mu S$.

Eigenvalues: $\mu_1 = 6.39 \times 10^6$, $\mu_2 = 8.14 \times 10^6 + 3.2 \times 10^8 j$, $\mu_3 = 8.14 \times 10^6 - 3.2 \times 10^8 j$, $\nu_1 = -9.46 \times 10^7$, $\nu_2 = 7.56 \times 10^6 + 3.23 \times 10^7 j$, $\nu_3 = 7.56 \times 10^6 - 3.23 \times 10^7 j$.

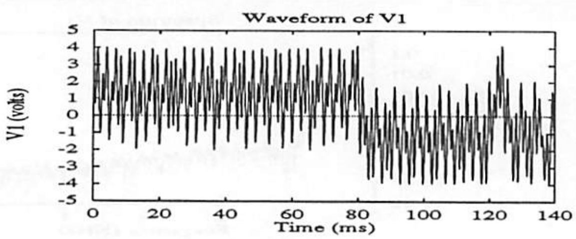

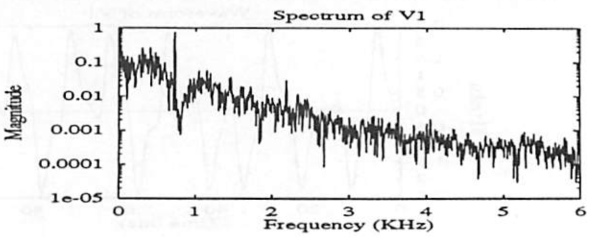

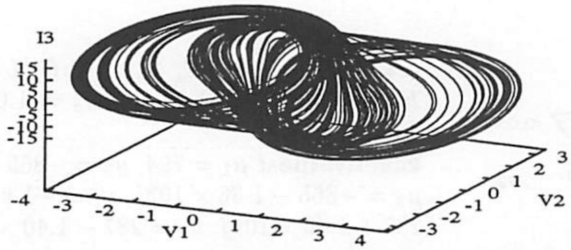

5.14 $C_1 = 269.6nF$, $C_2 = 1\mu F$, $L = 41.5mH$, $R = 1K\Omega$, $R_0 = -35.7\Omega$, $G_a = -2.764mS$, $G_b = 0.1805mS$.

Eigenvalues: $\mu_1 = 6.86 \times 10^3$, $\mu_2 = -226 + 4.65 \times 10^3 j$, $\mu_3 = -226 - 4.65 \times 10^3 j$, $\nu_1 = -4.84 \times 10^3$, $\nu_2 = 160 + 4.65 \times 10^3 j$, $\nu_3 = 160 - 4.65 \times 10^3 j$.

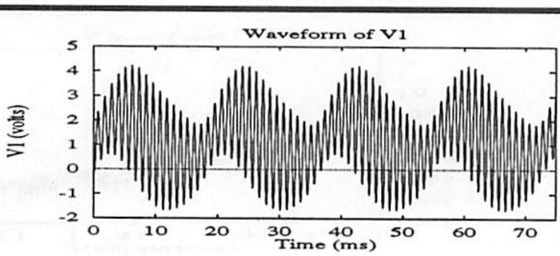

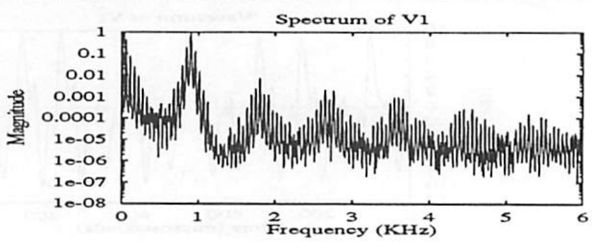

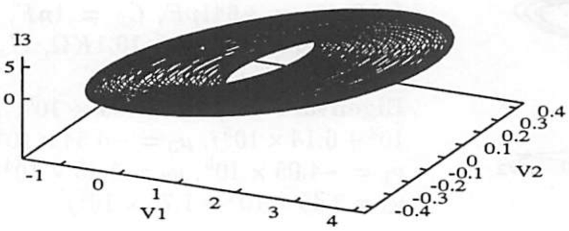

5.15 $C_1 = 31.72nF$, $C_2 = 1\mu F$, $L = 15.6mH$, $R = -1K\Omega$, $R_0 = 10.4\Omega$, $G_a = 0.9926mS$, $G_b = 1.023mS$.

Eigenvalues: $\mu_1 = 1.10 \times 10^3$, $\mu_2 = -226 + 5.70 \times 10^3 j$, $\mu_3 = -226 - 5.70 \times 10^3 j$, $\nu_1 = -781$, $\nu_2 = 195 + 5.65 \times 10^3 j$, $\nu_3 = 195 - 5.65 \times 10^3 j$.

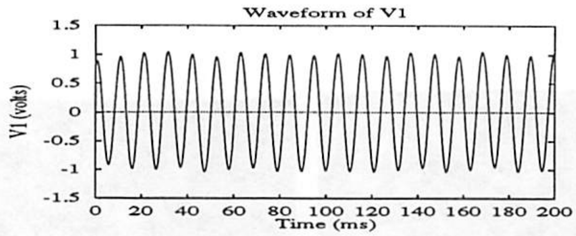

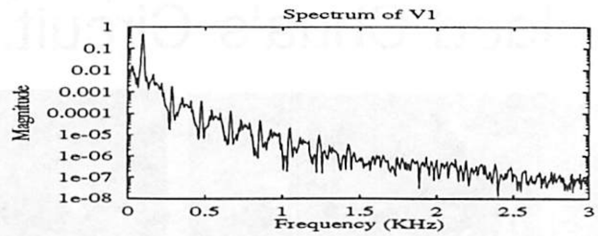

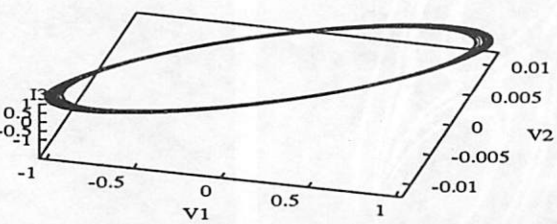

5.16 $C_1 = 9.98nF$, $C_2 = -1\mu F$, $L = 10.12mH$, $R = 1K\Omega$, $R_0 = 10.12\Omega$, $G_a = -0.99002mS$, $G_b = -0.9893mS$.
Eigenvalues: $\mu_1 = -1.6 \times 10^3$, $\mu_2 = 308 + 1.13 \times 10^3 j$, $\mu_3 = 308 - 1.13 \times 10^3 j$, $\nu_1 = 1.54 \times 10^3$, $\nu_2 = -1.31 \times 10^3 + 1.65 \times 10^3 j$, $\nu_3 = -1.31 \times 10^3 - 1.65 \times 10^3 j$.

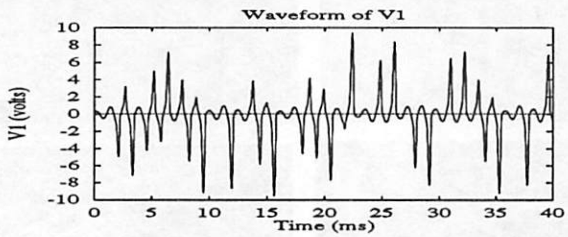

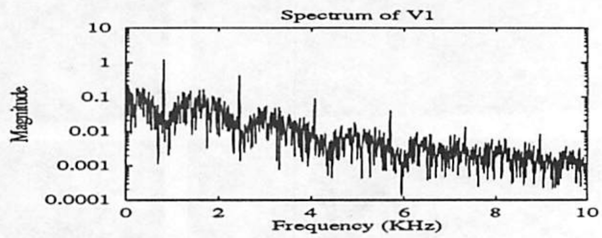

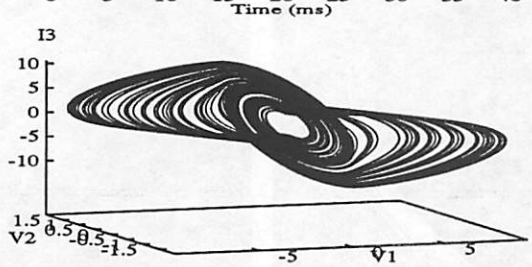

5.17 $C_1 = -13.33nF$, $C_2 = 1\mu F$, $L = 31.5mH$, $R = 1K\Omega$, $R_0 = -100\Omega$, $G_a = -2.4mS$, $G_b = -0.98mS$.
Eigenvalues: $\mu_1 = -1.04 \times 10^5$, $\mu_2 = 725 + 5.06 \times 10^3 j$, $\mu_3 = 725 - 5.06 \times 10^3 j$, $\nu_1 = 2.70 \times 10^3$, $\nu_2 = 489 + 1.02 \times 10^3 j$, $\nu_3 = 489 - 1.02 \times 10^3 j$.

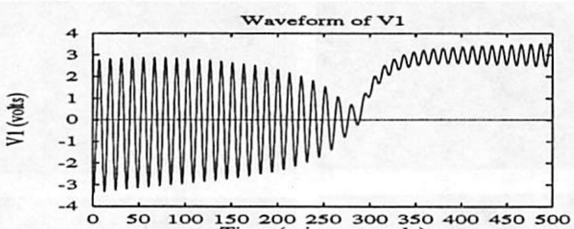

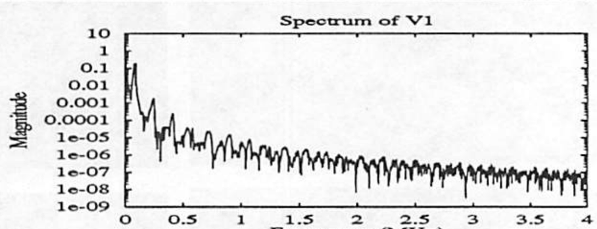

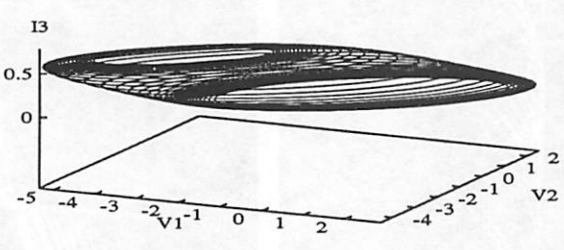

5.18 $C_1 = -621.5pF$, $C_2 = 1nF$, $L = 14.2mH$, $R = 1K\Omega$, $R_0 = 4.22K\Omega$, $G_a = -0.1392mS$, $G_b = -0.2175mS$.
Eigenvalues: $\mu_1 = 1.61 \times 10^4$, $\mu_2 = -3.68 \times 10^4 + 4.36 \times 10^5 j$, $\mu_3 = -3.68 \times 10^4 - 4.36 \times 10^5 j$, $\nu_1 = -4.46 \times 10^4$, $\nu_2 = 3.25 \times 10^3 + 5.86 \times 10^5 j$, $\nu_3 = 3.25 \times 10^3 - 5.86 \times 10^5 j$.

Table 6

Gallery of selected strange attractors from Unfolded Chua's Circuit.